Alternative Methods and Improvements to Current Delivery of Continuous Positive Airway Pressure for Treating Obstructive Sleep Apnea

By

Kelvin Duong

A thesis submitted in partial fulfillment of the requirements for the degree of

Master of Science

Department of Mechanical Engineering

University of Alberta

Abstract

For adults, the standard treatment for obstructive sleep apnea (OSA) is the delivery of continuous positive airway pressure (CPAP) through nasal/facial masks. For children, CPAP therapy is used if adenotonsillectomy is not a viable option or if OSA persists after surgery. By acting as a pneumatic stent, CPAP can prevent the collapse of the upper airways, thus restoring breathing and sleep. Though effective, tight-fitting CPAP masks can be uncomfortable to patients, contributing to adherence concerns. Recently, several groups have been investigating alternative methods of treatment to improve adherence to CPAP. One method is the delivery of CPAP through customized nasal/facial masks. Another method is generating positive airway pressures using nasal high flow (NHF) therapy. Both methods seek to improve comfort of OSA treatments, and therefore potentially increase adherence. This thesis aims to add greater insight into alternatives and improvements to current OSA treatments.

The feasibility of delivering CPAP through customized nasal masks were demonstrated by assessing mask leakage and comfort and comparing them to commercially available CPAP nasal masks. Customized masks, fabricated using 3D facial scanning and modern additive manufacturing process, were assessed against three different sizes of commercial masks (petite, small/medium, and large) from the same supplier in a cross-over study involving six healthy adult volunteers. Mask leakage and comfort were evaluated for varying CPAP levels (4 cmH_2O. 8 cmH_2O, and 12 cmH_2O) and mask tightness (loose – 100 g, appropriate – 350 g, and tight – 600 g). Leak was measured in real time using an inline low-resistance Pitot tube flow sensor, and each mask was ranked for comfort by the subjects.

As expected, mask leak rates varied directly with CPAP level and inversely with mask tightness. The petite mask yielded the highest mask leaks and was ranked least comfortable by all subjects. Relative mask leaks and comfort rankings for the other commercial and customized masks varied between individuals. Three participants found their customized masks to be most comfortable, whereas the other three participants found a commercial sized mask most comfortable. The mask leak rates between each participants' customized masks were comparable to the leak rates of their preferred commercial sized masks. At an appropriate fit, fit typically tightened to for night use, the customized nasal masks were able to deliver target CPAP levels in all six participants without triggering any alarms on the CPAP machine. This demonstrates the feasibility of using customized nasal masks as an alternative to commercial manufactured ones.

With a focus on children, NHF therapy was investigated as an alternative treatment option to CPAP. Positive airway pressures and gas washout were compared between the two therapies in 10 nasal airway replicas, built based on computed tomography scans of children aged 4 to 8 years. NHF was tested at a single flow rate of 20 L/min, and CPAP was tested at two CPAP levels, 5 and 10 cmH_2O. NHF was delivered with three different high flow nasal cannula models provided by the same manufacturer, and CPAP was delivered with a sealed mask. A lung simulator was used to establish tidal breathing in each replica, and airway pressure at the trachea was recorded over time. For gas washout measurement, end tidal carbon dioxide ($EtCO_2$) was measured at the trachea with a capnograph, while carbon dioxide was being injected at the lung simulator. Changes in $EtCO_2$ compared to baseline values (no intervention) were assessed.

NHF therapy generated positive end-expiratory pressures (PEEP) ranging from 3.5 to 5.4 cmH_2O across the three nasal cannulas, similar to a PEEP of 4.9 cmH_2O generated by CPAP at a setting 5 cmH_2O. Variation in tracheal pressure was higher between airway replicas for NHF

compared to CPAP. $EtCO_2$ decreased from baseline during administration NHF, whereas it increased during CPAP. No statistical difference in tracheal pressure nor $EtCO_2$ was found between the three high flow nasal cannulas. This demonstrates that NHF therapy can generate positive airway pressures similar to lower end CPAP settings used in children, with the added benefit of gas washout.

Both customized nasal masks and NHF therapy through nasal cannulas are feasible alternative methods to current CPAP treatments. Both methods may potentially improve comfort and increase adherence, and they may provide a treatment option to those who are CPAP-intolerant or have craniofacial abnormalities.

Preface

This thesis contains work that has been co-authored, some has been published and some will be submitted for publication. Chapter 2 is currently published as: "Feasibility of three-dimensional facial imaging and printing for producing customised nasal masks for continuous positive airway pressure" ERJ Open Research 2021 7: 00632-2020; DOI: 10.1183/23120541.00632-2020. I was the primary author for this manuscript. Co-author contributors were Joel Glover, Alexander C. Perry, Deborah Olmstead, Dr. Mark Ungrin, Dr. Pina Colarusso, Dr. Joanna E. MacLean, and Dr. Andrew R. Martin. The design and manufacture of the customized nasal masks were done by Joel Glover and Alexander C. Perry. I was responsible for setting up the experimental apparatus used to measure mask leak which utilized a LabVIEW script specifically created for this work. My responsibilities also included running the *in vivo* experiments with the assistance of Deborah Olmstead. Chapter 3 was also a co-authored manuscript where I was the primary author and will be submitted for publication in a scientific journal. Co-author contributors were Dr. Michelle Noga, Dr. Warren H. Finlay, Dr. Joanna E. MacLean, and Dr. Andrew R. Martin. Printed replicas used in this chapter were derived from CT scan data provided by Dr. Noga and printed by Tyler J. Paxman. I was responsible for experimental set-up and conducing the *in vitro* experiments. The analysis done for both chapters 2 and 3 were done using MATLAB scripts that were written specifically for each work. Finally, the drafting of both manuscripts was my responsibility with significant editorial support, direction, and contributions from Dr. Martin as well as the co-authors listed for each chapter.

Acknowledgements

I would like to start by expressing my gratitude to my remarkable supervisor, Dr. Andrew Martin. When I was an undergraduate, I was given the opportunity to work under his supervision as a summer research student. My time during those four months greatly sparked my interest in academia and research, especially in the field of respiratory fluid mechanics, which ultimately led to my decision to purse a Master's degree. Without his support, I would not have been able to present this work. His guidance, patience, and knowledge has made my graduate student experience a very enjoyable and rewarding one. Dr. Martin is the best supervisor/teacher I could have ever asked for, and I would not trade this experience for any other.

I would like to thank my other co-authors, Joel Glover, Alexander Perry, Deborah Olmstead, Dr. Mark Ungrin, Dr. Pina Colarusso, Dr. Joanna MacLean, Dr. Michelle Noga, and Dr. Warren Finlay, for their hard work and contributions on the work that is presented in this thesis. Without their support and expertise, the works in this thesis would not be what they are.

I would like to express my appreciation to other members of Dr. Martin and Dr. Finlay's research groups, John Chen, Paul Moore, Tyler Paxman, Kineshta Pillay, Cole Christianson, Scott Tavernini, and Conor Ruzycki. Over my graduate studies, their advice and support in both the technical aspects of research and graduate course work has been invaluable in helping me navigate through my degree. I would like to also thank Helena for her assistance over the years in preparing the equipment I needed to complete my work. She was very helpful whenever I ran into experimental issues, and she is fondly remembered.

I am very grateful for my parents who have been so supportive of at every stage of my education. Their encouragement has made pursing my passion all that more rewarding.

Finally, I would like to acknowledge the financial assistance from the Alberta Economic Development and Trade, Research and Innovation Seed Grant from Respiratory Health Strategic Clinical Network (Alberta Health Services), the Lung Association Alberta & NWT, National Grant Review, and Fisher & Paykel Healthcare. Their financial assistance made the work in this thesis possible.

Table of Contents

List of Tables

List of Figures

Chapter 1: Introduction

1.1 Overview

Obstructive sleep apnea (OSA) is a common sleep breathing disorder that is characterized by partial or complete interruptions in breathing caused by obstruction of the upper airways. OSA cases can range from mild to severe (Shapiro and Shapiro, 2010). Observable symptoms of OSA include loud snoring, witnessed apneas, and choking (Sigurdson and Ayas, 2007). In the short term, a common negative health consequence is excessive daytime sleepiness, which has been linked to increased motor vehicle accidents (Donovan *et al*., 2015; Shapiro and Shapiro, 2010). Daytime sleepiness has also been linked to decreased work productivity and consequent economic losses and burdens (Léger and Stepnowsky, 2020; Mulgrew *et al*., 2007). In the long term, moderate to severe OSA has been associated with an increased risk of medical comorbidities including hypertension, stroke, coronary artery disease, and congestive heart failure (Phillips, 2005). Negative impacts on cognitive functioning caused by excessive daytime sleepiness are more serious in children than in adults. Decreased learning, attention span, and behavioural capabilities are some of the impacts to cognitive function in children that have been associated with aggressive behaviours in the classroom, poor test performance, and poor problem-solving skills (Alsubie and BaHammam, 2017; Bhattacharjee *et al*., 2009; Gozal and O'Brien, 2004). Another negative consequence seen only in children with OSA is a reduction in weight gain and growth (Alsubie and BaHammam, 2017; Gozal and O'Brien, 2004). Moderate to severe OSA is estimated to affect 13 % of men and 6 % of women (Peppard *et al*., 2013). In children, OSA is estimated to affect 1 to 10 % (Alsubie and BaHammam, 2017; Andersen, Holm, & Homøe, 2016; Chan, Edman, & Koltai, 2004; Marcus *et al*., 2012).

The current standard therapy for treating OSA in adults is the delivery of continuous positive airway pressure (CPAP). In children, adenotonsillectomy is the first line therapy for OSA, but if surgery is not viable or if OSA persists afterwards, then CPAP therapy is an option that is used (Marcus *et al*., 2012). CPAP, generally delivered through a tight-fitting mask, keeps the upper airways open by acting like a pneumatic stent. This action restores breathing during sleep, reversing daytime effects and reducing long-term OSA-related health consequences (Donovan *et al*., 2015; Rotenberg, Murariu, & Pang, 2016; Shapiro and Shapiro, 2010; Weaver and Sawyer, 2010). Although CPAP therapy is effective in treating OSA, adherence to it is a major issue. Adherence, commonly defined by researchers as use of CPAP ≥ 4 hours/night for ≥ 70 % of nights (Shapiro and Shapiro, 2010; Weaver and Sawyer, 2010), ranged from 30 – 60 % in adults (Rotenberg, Murariu, & Pang, 2016; Weaver and Sawyer, 2010) and from 33 – 75 % in children (Hawkins *et al*., 2016; Machaalani, Evans, & Waters, 2016; Nixon *et al*., 2011). Many factors have been investigated in determining CPAP adherence. Discomfort is one factor that has been linked to poor CPAP adherence (Salepci *et al*., 2013; Valentin *et al*., 2011). During treatment, the headgear is often tightened excessively to reduce mask leakage in order to ensure that CPAP is being delivered at target settings. This tightening typically leads to discomfort, skin breakdown, and pressure sores where the mask contacts the face (Massie and Hart, 2003; Shapiro and Shapiro, 2010). On the other hand, improper tightening of the mask can lead to ineffective treatment and mask leakage. Mask leakage can cause discomfort in patients through deleterious effects such as loud noise levels and eye irritations (Massie and Hart, 2003; Shapiro and Shapiro, 2010). Another issue with current CPAP treatment affects those with craniofacial abnormalities, especially children. Children with craniofacial abnormalities experience a higher incidence of OSA than children without (Rosen, 2011). However, these children tend to have difficulties

using commercially available CPAP masks because they may not fit properly onto their facial structures. Thus, alternative options are required.

In recent years, there have been several groups looking into alternative methods of treatment to improve adherence to OSA therapies. Customized masks and mask cushions as alternatives to commercially available ones have been investigated, yielding positive results. A study by Cheng *et al* found that their own customized nasal mask cushions provided a better fit and required less applied force on the headgear than conventional cushions while also yielding similar leak rates (Cheng *et al*., 2015). Morrison *et al* found their customized oronasal mask decreased mask leakage, improved AHI, and improved adherence for a child test subject with craniofacial abnormalities (Morrison *et al*., 2015). Nasal high flow (NHF) therapy has been shown to generate positive airway pressures (Parke, McGuinness, & Eccleston, 2009). For this reason, several groups have also researched NHF therapy as an alternative to CPAP therapy. In studies by Hawkins *et al* and Amaddeo *et al*, both groups found that NHF therapy resulted in better compliance and fewer respiratory events in children who were intolerant to standard CPAP therapy (Amaddeo *et al*., 2019; Hawkins *et al*., 2017). More research into alternatives and improvements to standard CPAP therapy is warranted to combat the problem of adherence and help provide solutions to those who struggle or are unable to use current treatments.

1.2 Mechanisms of Continuous Positive Airway Pressure and Nasal High Flow Therapy

As mentioned in the previous section, the delivery of CPAP restores breathing in those with OSA by acting as a pneumatic stent. During CPAP therapy, a CPAP machine generates varying flow rates of air (arrow 1, Figure 1.1) which are adjusted according to the pressure monitored at the outlet of the CPAP machine, and are delivered to the patient through a supply tube/hose via a nasal/facial mask. Large-bore supply tubing is used to minimize pressure drop between the CPAP machine and the mask. The supply tube has an expiratory port on it, which acts both as an exit for a patient's expired air, as well as an orifice that helps maintain a constant pressure in the system. For a given CPAP setting, there is an associated flow rate of air through the expiratory port that is required to achieve and maintain that pressure in the system (arrow 2, Figure 1.1). The pressure in the system is a function of the flow rate exiting the expiratory port, e.g., if the flow rate through the port decreases, so will the pressure being delivered. During breathing, the flow rate through the expiratory port would tend to decrease or increase with respect to either inspiration or expiration (arrow 3, Figure 1.1). This would cause the pressure being delivered to change. To compensate, the CPAP machine adjusts the provided flow rate to maintain a constant pressure in the supply tubing, which has the effect of maintaining a constant flow rate out of the expiratory port. Sometimes during exhalation, the magnitude of airflow may be greater than that required through the expiratory port to maintain the target CPAP level, so backflow will occur (arrow 4, Figure 1.1). Finally, in the presence of mask leaks (arrow 5, Figure 1.1), the flow rate out of the expiratory port would tend to decrease, so the CPAP machine increases the flow rate it provides in order to offset the loss out of the system due to this unintended mask leak, and thereby maintain target pressure. However, the CPAP machine's ability to adjust the provided

flow rates for a given CPAP setting is limited. Thus, if the mask leaks are too large, the CPAP machine will not be able to fully compensate and effective therapy will not be achieved. In this case, the CPAP machine will typically trigger a 'high leak' alarm.

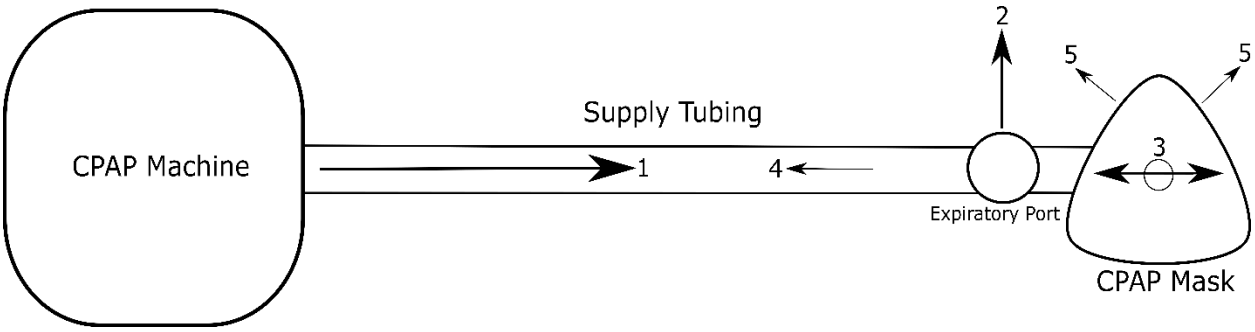

Figure 1.1: Schematic of CPAP therapy with arrows indicating the flow direction of air. (Arrow 1) Flow of air provided by the CPAP machine. (Arrow 2) Flow of air that exits the expiratory port on the supply tube. (Arrow 3) Flow of air from the patient during inspiration or expiration. (Arrow 4) Backflow of air that may occur during expiration. (Arrow 5) Flow of air out of the mask when there are sources of leaks. CPAP: Continuous positive airway pressure

For NHF therapy, a constant flow rate of air is provided by a flow controller, at rates intended to be higher than normal inspiration flow rates, to a patient through a NHF cannula (Figure 1.2). The delivery of NHF helps patients by providing washout of the nasopharyngeal dead space, which improves the efficiency of gas exchange, and has been shown to decrease the work of breathing (Dysart *et al*., 2009). As mentioned in the previous section, the delivery of NHF has also been shown to generate postive airway pressures, leading researchers to investigate it as an alternative option to CPAP therapy (Parke, McGuinness, & Eccleston, 2009). However, a key difference between NHF therapy and CPAP therapy, is the lack of pressure monitoring during NHF therapy, such that flow rates delivered by the NHF machine are constant, and are not controlled in response to pressure. Furthermore, the NHF breathing circuit contains no expiratory

port, such that the leak path is formed by the fit of cannula prongs into the patient's nostrils. Accordingly, airway pressures delivered to patients at a set NHF supply flow rate are not monitored, and are difficult to predict.

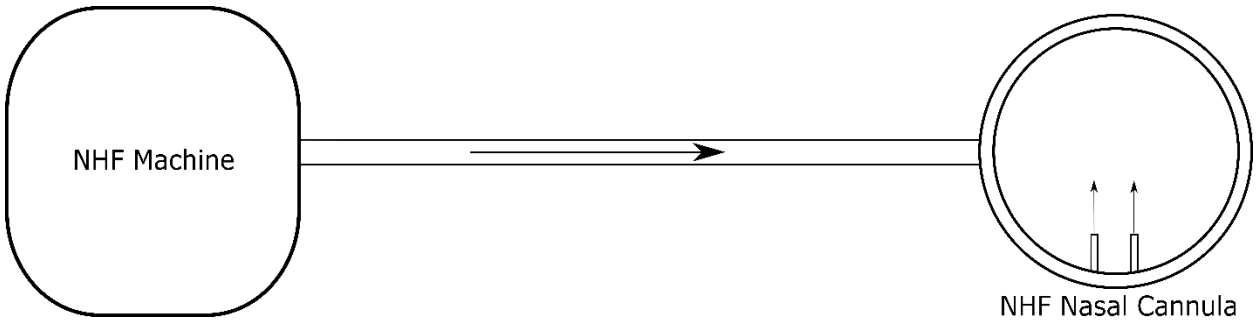

Figure 1.2: Schematic of nasal high flow therapy.

1.3 Research Objective

The objective of this thesis is to contribute to current literature on alternatives to, and remediation of problems associated with, standard CPAP therapy. The first solution investigated is the use of customized nasal masks manufactured with 3D facial scanning and modern additive processes. The customized nasal masks were assessed against commercially available ones in a feasibility study involving six healthy adult volunteers. The study tested a range of masks, mask tightness, and CPAP settings. Mask leakage was measured to determine the ability of the customized masks to safely deliver and maintain target CPAP levels. Comfort was also assessed to determine whether or not customized masks were easier to wear and might thereby help improve adherence to treatment.

The second solution is the use of NHF therapy through nasal cannulas. NHF therapy was assessed against CPAP therapy in an *in vitro* study involving upper airway replicas of 10 children aged 4 to 8 years. Tracheal pressures were measured to correlate positive airway

pressures generated by NHF therapy with pressures generated by CPAP therapy. NHF is known to reduce rebreathing of expired air due to the washout of the nasopharyngeal dead space (Dysart *et al*., 2009). Therefore, end-tidal carbon dioxide ($EtCO_2$) was examined between the two therapies to observe the effects of CPAP on carbon dioxide washout. Multiple nasal cannulas were also investigated to explore the influence cannula choice had on generated positive airway pressures and washout for this age group.

Lack of adherence is a major concern for current CPAP therapy. Results from this research may add valuable insight into alternatives and improvements to CPAP therapy that could help increase adherence. Customized nasal masks and NHF therapy through nasal cannulas may also be beneficial to those with craniofacial abnormalities, especially children who either struggle to use or are intolerant to standard CPAP treatment. The experimental evaluation of these alternatives is the focus of this thesis.

1.4 Thesis Structure

The thesis is presented in four chapters. The first (current) chapter presents background information on OSA and the main objectives of the research. This background information includes details of the disorder, current treatment and its issues, and alternatives and solutions being researched. The second chapter describes a feasibility study examining customized nasal masks as an alternative to commercially available ones for delivering CPAP. Mask leakage and comfort were assessed for both commercial and customized masks in six healthy adult volunteers with a range of CPAP settings and mask tightness. The third chapter details an *in vitro* study investigating NHF therapy as an alternative to CPAP. Tracheal pressures and $EtCO_2$ were

measured in upper airway replicas modeled from 10 children aged 4 to 8 years. Tracheal pressures provide information on whether or not NHF can generate positive airway pressures comparable to those of CPAP when used in this age group. The final chapter provides a summary of the main findings and explores potential future work on this research.

Chapter 2: Feasibility of 3-Dimensional Facial Imaging and Printing for Producing Customized Nasal Masks for Continuous Positive Airway Pressure

A version of this chapter has been published in ERJ Open Research 2021 7: 00632-2020; DOI: *10.1183/23120541.00632-2020.*

2.1 Introduction

Obstructive sleep apnea (OSA) is a common sleep-related breathing disorder where individuals experience partial or complete interruptions in breathing due to obstruction of the upper airways. Moderate to severe OSA, defined in adults as an apnea-hypopnea index (AHI) ≥ 15/hour (Donovan *et al*., 2015), has been linked to significant negative health consequences, ranging from daytime sleepiness in the short term to acute cardiovascular events and increased risk of a range of medical comorbidities in the long term (Shapiro and Shapiro, 2010). Increased motor vehicle accidents have also been linked to individuals experiencing excessive daytime sleepiness (Donovan *et al*., 2015; Shapiro and Shapiro, 2010). It is estimated that 13 % of men and 6 % of women have moderate to severe OSA (Peppard *et al*., 2013).

Currently, the standard treatment for OSA in adults is the delivery of continuous positive airway pressure (CPAP). CPAP acts as a pneumatic stent to prevent collapse of the upper airway during sleep, thus restoring breathing and sleep, and reducing OSA-related health consequences (Donovan *et al*., 2015; Rotenberg, Murariu, & Pang, 2016; Shapiro and Shapiro, 2010; Weaver and Sawyer, 2010). Administration of CPAP requires a tight-fitting interface, normally a mask, which should fit the individual patient's facial structure (Strickland, 2019). Mask air leakage and discomfort have been linked to poor CPAP adherence (Salepci *et al*., 2013; Valentin *et al*., 2011). Mask leak can cause deleterious effects, such as eye irritation and high noise levels

(Massie and Hart, 2003; Shapiro and Shapiro, 2010). Conversely, when mask leak is reduced through excessive tightening of the headgear, discomfort such as pain, rashes, skin breakdown, and pressure sores may arise where the mask contacts the face (Massie and Hart, 2003; Shapiro and Shapiro, 2010). Improving the CPAP mask fit, such that mask leakage is minimized at a comfortable tightness of fit, may help improve access to CPAP therapy for a more diverse range of patients, and could potentially increase adherence to CPAP therapy.

To improve CPAP or non-invasive ventilation (NIV) mask fit, several groups have recently investigated the manufacture of customized masks or mask cushions using a combination of 3D facial scanning and modern additive manufacturing processes (Cheng *et al*., 2015; Morrison *et al*., 2015; Sela *et al*., 2016; Shikama *et al*., 2018). Such approaches may be particularly useful for individuals with OSA and craniofacial anomalies (Morrison *et al*., 2015). In one comparison between customized masks and a conventional commercial mask, subjects with severe OSA showed improved AHI compared to their baseline when using the customized mask versus subjects who used a commercial mask over a 14-day period (Cheng *et al*., 2015).

Here, we report on the development of individualized, custom-built nasal CPAP masks using 3D facial scanning and 3D printing technologies. Mask leakage and comfort were evaluated in healthy, adult volunteers for customized masks and commercial masks of three different sizes in a cross-over study.

2.2 Methods

This feasibility study of custom masks for non-invasive delivery of CPAP was conducted at the Respiratory Fluid Mechanics Lab at the University of Alberta in Canada between February 2019 and June 2019. The study was approved by the University of Alberta Research Ethics Board (Study ID: MS1_Pro00085707) and subjects provided informed written consent.

2.2.1 Subjects

Each subject enrolled in the study was at least 18 years old and was a non-smoker. Six subjects were enrolled in this feasibility study. Non-probability, purposive sampling was used to select a useful group of subjects, based on their motivation, willingness to participate, and capability to effectively communicate their experiences and opinions (Daniel, 2012). There were four male subjects and two female subjects, aged 24 - 62 y. No subjects had previously used nocturnal CPAP support.

2.2.2 Experimental Apparatus

In this study, four different CPAP masks were tested. This included three different sizes of a commercial CPAP mask (Wisp Nasal CPAP Mask; Philips Respironics, Murrysville, PA; petite, small/medium, and large) along with a customized CPAP mask designed and individually manufactured for each subject (Live Cell Imaging Laboratory at the University of Calgary, Alberta, Canada). The Wisp masks were selected because they fit a wide range of facial geometries, and three sizes were tested to provide comparative data ranging from a poor fit to a good fit in each subject. During the study, each subject wore standard headgear (Fabric Frame; Philips Respironics, Murrysville, PA). The mask was connected to a supply tube which was connected to a CPAP machine (S8 Elite; ResMed, San Diego, CA) with a viral/bacterial filter

(VP7100; KEGO Corporation, London, Ontario, Canada) and an inline Pitot tube flow sensor (RespEQ, Baltimore, MD; Figure 2.1). The Pitot tube flow sensor was used to obtain mask air leak values in real time by measuring the airflow, in standard litres per minute (SLPM; with standard conditions defined as 21.1 ºC and 101.3 kPa), between the CPAP machine and the mask. The Pitot tube flow sensor was selected over a conventional pneumotach due to its low flow resistance, limiting the effects it had on the delivery of CPAP (Kirkness *et al*., 2011). A pressure transducer (Seleon, Heilbronn, Germany) was used to convert the differential pressure across the sensor into an electric signal which was transmitted using a microcontroller board (UNO Rev3; Arduino, Somerville, MA) and recorded with LabView software (National Instruments, Austin, TX). The flow sensor-pressure transducer combination was calibrated ahead of the study against a series of known airflow rates, ranging from -120 to 120 SLPM. Time-averaged airflow rate was obtained by analyzing the airflow data with the program MATLAB (MathWorks, Natick, MA). Before each subject visit, the intentional air leak through the expiratory port of the supply tubing was measured at a CPAP setting of 4, 8, and 12 cmH_2O using the Pitot tube flow sensor with the end of the tube sealed off. Mask air leak was then later calculated after completion of each subject's test by subtracting the intentional air leak from the time-averaged airflow.

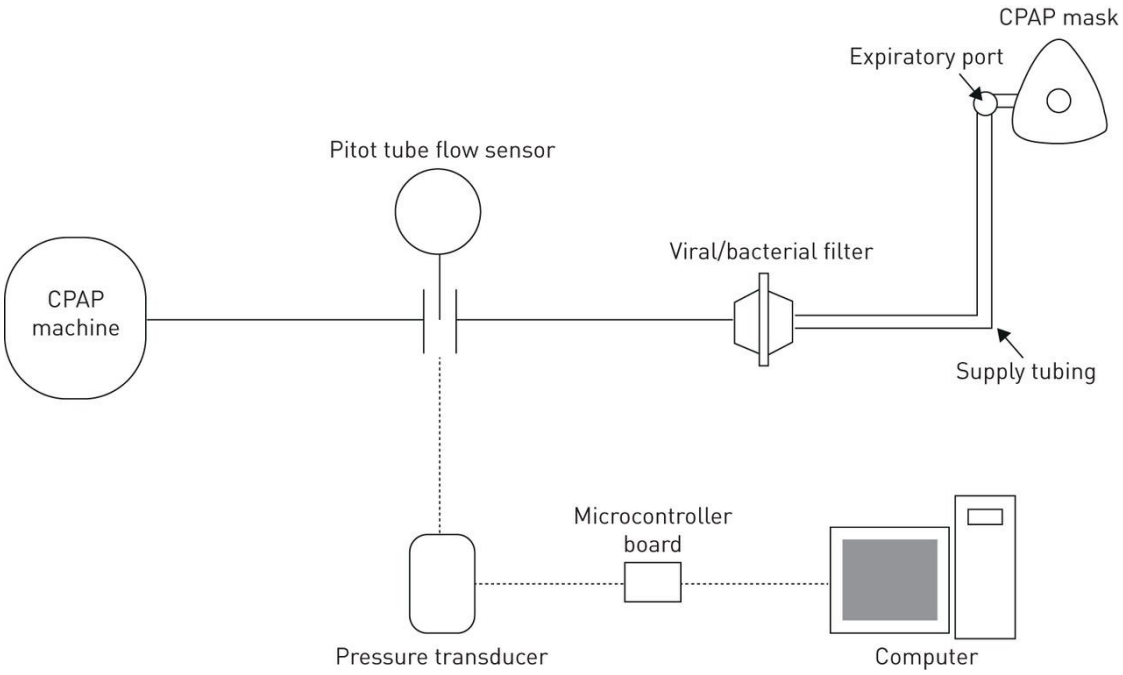

Figure 2.1: Schematic of experimental apparatus. CPAP: continuous positive airway pressure

2.2.3 Fabrication of Custom Masks

The CPAP mask design consists of two components, a standard coupler and a customized cushion fit to the individual face (Figure 2.2). The coupler was designed to connect the cushion to the commercial headgear and supply tubing (Philips Respironics, Murrysville, PA). The coupler is a hard-plastic component and was fabricated using a stereo-lithography apparatus 3D printer (Peopoly Moai, Los Angeles, CA) using ultraviolet curable resin. The same coupler design was used for all custom masks that were tested. All six customized cushions are shown in Figure 2.3.

Figure 2.2: Final customized mask. (A) Portion of mask labelled "coupler" (front) interfaces with the headgear and hosing that conducts positive pressure from the CPAP machine. The "cushion" (back) contacts the subject's face. (B) Demonstration of the coupler attached to the headgear and hosing of the Wisp CPAP system. (C) Customized mask worn in situ.

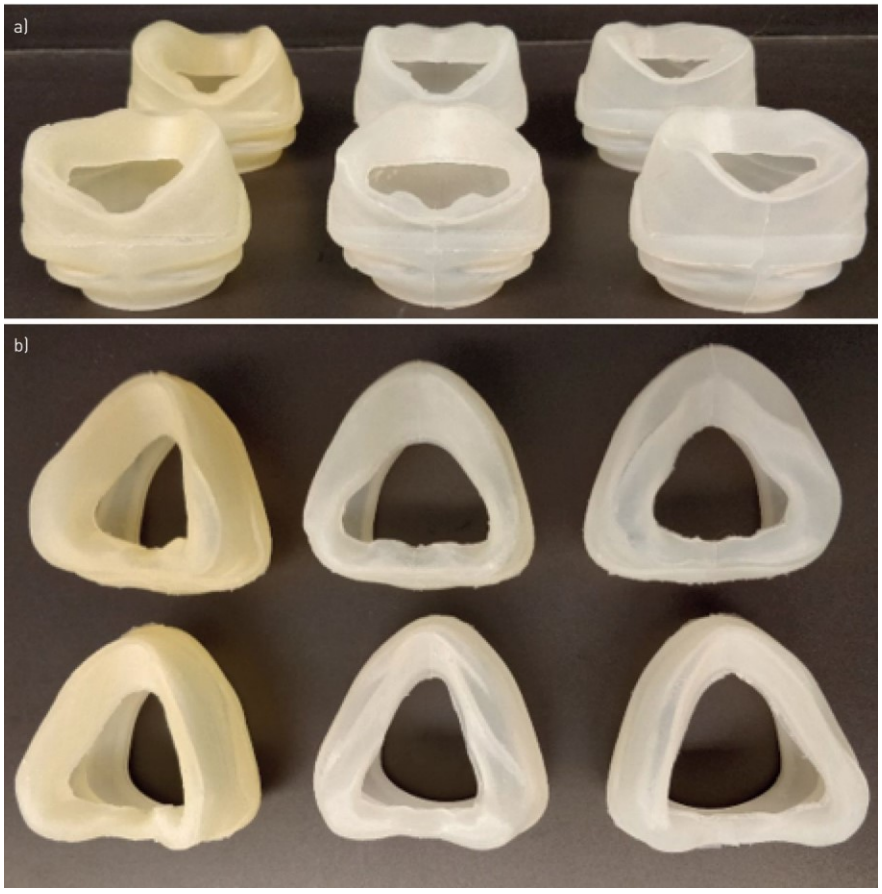

Figure 2.3: (A) Top down view of all six customized cushions. (B) Front view of all six customized cushions.

Subjects' facial features were captured using a 3D facial scanning system (3dMDFace System, Atlanta, GA). The facial scans were digitally edited to limit the regions examined (frontal, nasal, infraorbital, buccal, and mental regions) using Autodesk Meshmixer (San Rafael, CA). The edited scans were imported into computer aided design software to design custom cushions to match the facial features (Autodesk Fusion 360, San Rafael, CA).

The cushion-skin interface was customized by point-wise matching the surface of the cushion, which contacts the skin, to the scanned mesh of corresponding facial features. To ensure skin safety and comfort, the cushions were fabricated from a skin safe silicone (Smooth-on Dragon Skin 30, Macungie, PA). As this material could not be printed directly using available 3D printers, it was cast into 3D printed molds. Using a Constructive Solid Geometry (CSG) approach, the desired cushion geometry was subtracted from the mold box interior, leaving a shell in the shape of the custom cushion between an inner and outer mold component (Figure 2.4, A). These components were manufactured using a fused filament fabrication 3D-printer (Ultimaker 3, Utrecht, The Netherlands) using 2.85 mm polylactic acid filament (Filaments.ca 6B14 FCAPLA2BK, Mississauga, ON, Canada). The 3D-printer used has a manufacturer-reported accuracy of ± 12.5 μm XY (i.e. in the plane parallel to the print bed) and ± 2.5 μm Z (normal to the print bed). The mold box was assembled and clamped, two-component silicone was prepared as per the manufacturer's instructions and injected into the mold box using a 60 mL Luer-lock syringe. After curing (16 hr, 20˚C), the cushion was removed from the mold and visually inspected for tears and other sources of unintended leak prior to bench testing. In two instances, cushions failed visual inspection due to the presence of air pockets, which was attributed to inadequate material being injected. These cushions were rejected and remade for use in the present study.

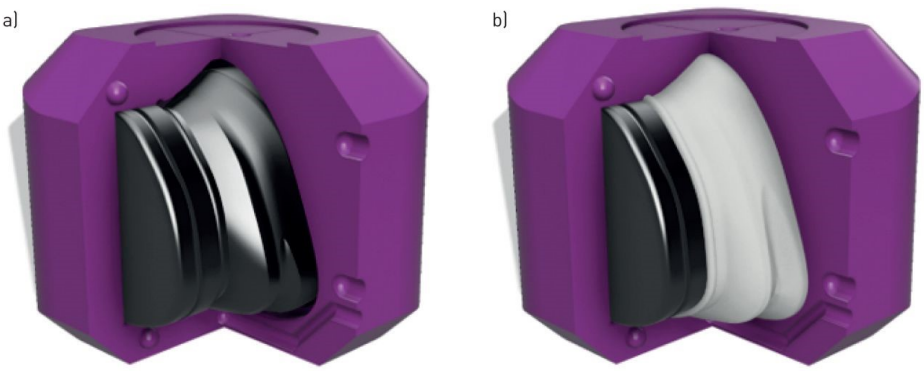

Figure 2.4: (A) Assembled mold box components with one component removed for visualization. Outer mold shown in magenta, inner mold shown in black. (B) Demonstration of custom cushion created after injection of cavity with silicone (white).

2.2.4 Study Design

This feasibility study aimed to investigate the use of customized 3D printed CPAP masks through comparison of mask air leak rates and subject-reported comfort rankings against commercially available CPAP masks.

For each study subject, the headgear was adjusted to obtain three levels of mask tightness, each within a 50 g tolerance, that were measured by the force applied to the face: 100 g for a loose fit, 350 g for an appropriate fit, and 600 g for a tight fit. These forces were measured using a force gauge (Model DFG35-10; OMEGA, Norwalk, CT). The mask tightness chosen to represent loose, appropriate, and tight fits were determined in preliminary consultation and lab bench testing with a nurse practitioner highly experienced in fitting CPAP masks to patients. The appropriate fit was determined using the "two-finger rule" (Castro-Codesal, Olmstead, & MacLean, 2019). Three CPAP pressures were selected for testing: 4, 8, and 12 cmH_2O. This coincides with the median CPAP of 8 – 10 cmH_2O used in other OSA studies (Bakker, Neill, &

Campbell, 2012; Duarte *et al*., 2020; Guralnick *et al*., 2012; McArdle *et al*., 1999; Rowland *et al*., 2018; Shirlaw *et al*., 2019).

Each subject underwent testing of the four masks at each pressure level and mask tightness for a total of 36 individual tests. Each pressure was applied for one minute with the flow sensor recording the airflow over the same period. Subjects were instructed to breathe normally while in a seated position. At the completion of the mask testing, each subject was asked to rank the four CPAP masks in order of comfort level.

2.2.5 Statistical Analysis

Mask air leak was compared between all four CPAP masks using a three factor repeated measures Analysis of Variance (ANOVA) procedure along with Tukey post hoc analysis. Additionally, a three factor repeated measures ANOVA procedure was used to specifically compare the commercial CPAP nasal mask that each subject found most comfortable with their customized mask. The three compared factors were the CPAP mask, CPAP level, and mask tightness. Results with two-sided $P \leq 0.05$ were considered significant. Statistical analysis was performed with MATLAB software.

2.3 Results

Six subjects were enrolled in this study. The intentional air leak through the expiratory port for the three tested CPAP levels was found to be 14.0 ± 0.4 SLPM for 4 cmH_2O, 19 ± 1 SLPM for 8 cmH_2O, and 24 ± 1 for 12 cmH_2O (mean ± standard deviation; n = 6). When testing with a loose fit the CPAP machine would alarm “high leak”, indicating that target pressures were not maintained in the breathing circuit and mask. This occurred for two subjects using their

customized masks at the 12 cmH_2O CPAP setting; two and four subjects using the petite size commercial mask at 8 and 12 cmH_2O, respectively; two subjects using the small/medium size commercial mask at both 8 and 12 cmH_2O; and one subject using the large commercial mask at 8 cmH_2O. When testing with the appropriate fit, the "high leak" alarm was given only for one subject using the petite size commercial mask at 12 cmH_2O. For all other combinations of mask tightness and CPAP levels, the customized and commercial masks delivered and maintained target CPAP in all six adult subjects, with no alarms.

Average mask air leaks for each combination of mask tested, CPAP level, and tightness are displayed in Table 2.1. Each factor, CPAP mask, CPAP level, and mask tightness had influence on mask air leak. Significant influences on leak were also observed in all interactions between the three factors apart from the interaction between CPAP mask and CPAP level. From post hoc analysis, the individual CPAP masks were compared against one another for each CPAP level and mask tightness combination. The pairs of masks observed to be significantly different in air leak have been displayed in Table 2.2.

Table 2.1: Average mask air leak for varying CPAP mask, CPAP level, and mask tightness

		Average Mask Air Leak ± Standard Deviation (SLPM); n = 6		
		CPAP Level (cmH_2O)		
		4	8	12
CPAP Mask				
	Mask Tightness (g)			
Petite	100	27 ± 13	48 ± 15	60 ± 22
	350	9 ± 5	17 ± 9	27 ± 15
	600	2 ± 2	5 ± 2	8 ± 4
Small/Medium	100	17 ± 19	37 ± 23	44 ± 19
	350	3 ± 1	7 ± 4	13 ± 9
	600	1.1 ± 0.5	1.3 ± 0.5	3 ± 2

Large	100	19 ± 14	28 ± 16	29 ± 5
	350	5 ± 6	16 ± 16	18 ± 10
	600	3 ± 3	9 ± **7**	13 ± 11
Custom	100	9 ± 2	28 ± 11	45 ± 20
	350	5 ± 2	11 ± 3	18 ± 4
	600	5 ± 3	8 ± 4	11 ± 2

Table 2.2: Differences in air leak between masks for varying CPAP level and mask tightness

	CPAP Level (cmH2O)		
	4	8	12
Mask Tightness (g)			
100	No Differences	No Differences	P > L
350	No Differences	No Differences	P > SM
600	C > P	P, C > SM	P, C > SM

[*] *Definition of abbreviations:* P = Petite; SM = Small/Medium; L = Large; C = Custom
Mask pairings observed to have significantly different mask air leaks when $P < 0.05$ in Post Hoc analysis.

2.3.1 Mask Comfort

Out of the four masks tested, three of the six subjects found the customized mask to be the most comfortable, two subjects found it to be the second most comfortable, and one subject found it to be the third most comfortable. Excluding the customized mask, four subjects preferred the large sized commercial mask and two subjects preferred the small/medium sized commercial mask.

2.3.2 Preferred Commercial CPAP Mask vs Customized CPAP Mask

When comparing the mask air leak for each subjects' preferred commercial mask to their customized mask, the influence of both pressure level and mask tightness were statistically significant, but the influence of the mask itself was not. Significant influence on mask leak was only observed in the interaction between CPAP level and mask tightness.

Relative mask air leak was variable between subjects when comparing their preferred commercial masks against their customized masks (Figure 2.5; Appendix: Figures A1 and A2). Some subjects showed a decrease in mask leak when using their customized masks whereas other subjects showed an increase in mask leak.

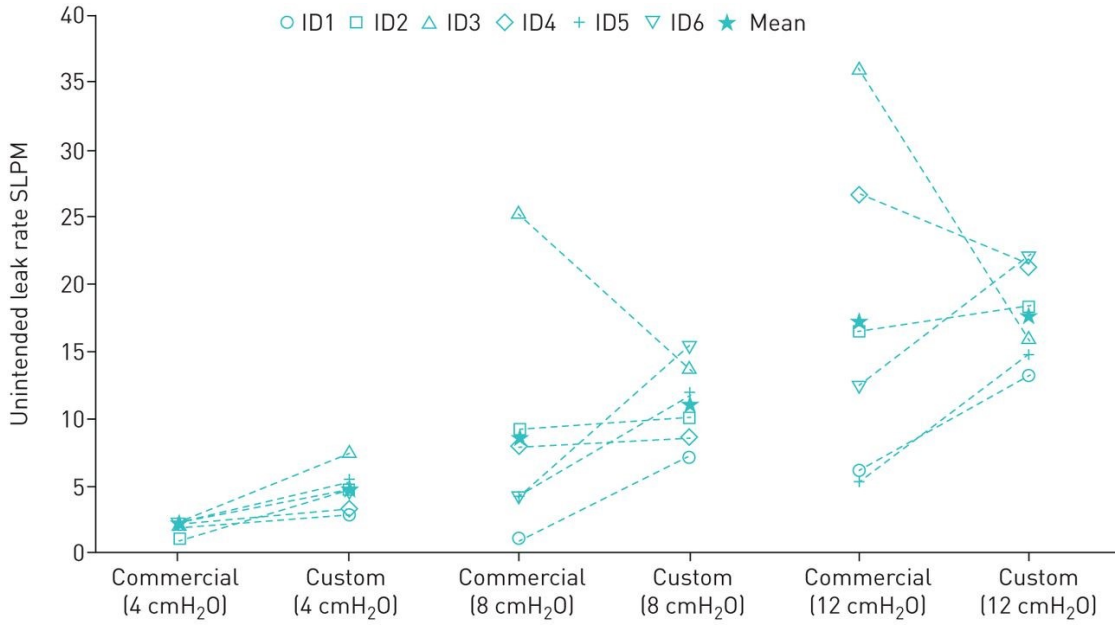

Figure 2.5: Mask air leak for each subject's preferred commercial CPAP mask and their customized counterparts at an appropriate fit (350 g). SLPM: standard litres per minute.

2.4 Discussion

Both mask leak and comfort results reported herein indicate that, on average, the customized nasal CPAP masks performed similarly to commercial masks (of appropriate size), for the small sample of healthy adults studied. For the tightness deemed appropriate, the customized masks did not produce any "high leak" alarm. These results suggest that customized masks could be used to deliver CPAP therapy safely and effectively. Conversely, customized masks did not consistently reduce mask leak nor improve comfort across study subjects. Rather, the relative leak and comfort between the customized masks and commercial masks were highly variable between subjects, presumably as a function of variable facial geometries. Methods of identifying individual patients most likely to benefit from provision of a customized CPAP mask have not been established.

Some limitations of the present feasibility study warrant comment. First, study subjects were in good health and had not previously required nocturnal CPAP support; therefore, they may not reflect patients who are prescribed CPAP. Results for commercial masks may represent a best-case scenario, as the subjects were all healthy without any craniofacial abnormality. Additionally, the commercial masks used in the present study do not necessarily reflect the best available mask for each individual across the broad supply of all masks available from various manufacturers. Future trials conducted in patients who are prescribed CPAP should compare customized masks with each patient's currently used commercial mask. Second, mask leak testing was done while each subject was seated at rest in an upright position with their head facing forward. Whether or not mask customization has an influence of variation in leak with body position, i.e. lying down or on one's side, or turning in bed, was not assessed in this study. Third, evaluation of all four masks was done in a single visit, which could have skewed comfort

rankings due to potential testing fatigue of wearing masks for the entire visit. To mitigate this factor, the order of the masks was randomized for each subject, as well as by providing a 10-minute recovery period between each mask tested. Fourth, though no significant difference was observed between customized and commercial masks in mask leak or in subject-reported comfort, these variables may not necessarily be similar between customized and commercial masks due the low power of the sample in this feasibility study. Finally, results presented here for customized masks are specific to the customized mask design and fabrication methods employed, including the silicone material used to form the portion of the mask which contacts the face. These results may not generalize to all methods of mask manufacturing.

Notwithstanding these limitations, two consistent trends were observed in the mask leakage data: mask leak varied directly with CPAP levels and inversely with mask tightness. In comparison between all masks, the petite-sized commercial mask exhibited the highest mask leak and was ranked least comfortable by all subjects. Further comparisons between the customized masks and the commercial mask that each subject ranked most comfortable showed no statistically significant influence of mask selection on measured mask leak, which is consistent with results for leakage reported by Cheng *et al.* (Cheng *et al*., 2015). Cheng *et al.* (Cheng *et al*, 2015.) reported leakage monitored by a CPAP machine over 14 days of use by patients with severe OSA randomized into groups using customized or commercial masks. Average (±SD) mask leak was 32 ± 19 l/min for customized masks versus 36 ± 48 l/min for commercial masks (Cheng *et al*., 2015). Although average mask leak was comparable between groups, variability in mask leak appeared notably lower for the group using customized masks. A similar reduction in variability was noted in the present work, particularly when masks were evaluated at the tightness of fit deemed appropriate.

Our study measured mask leakage in real time by using a low-resistance Pitot tube flow sensor. Other studies looking into customized CPAP masks obtained their leak data directly from the CPAP machine, which required overnight use to obtain an average leak rate (Cheng *et al*., 2015; Morrison *et al*., 2015). With mask leakage being the main comparative measurement made in the present study, measurements in real time allowed for rapid testing of varying masks, tightness, and CPAP levels. This allowed for faster evaluation of mask leakage between the tested variables. However, unlike the other studies where AHI was an important comparative measurement, our study did not assess AHI since overnight mask usage was not conducted.

Based on the comfort rankings, half of the subjects ranked the customized mask most comfortable, with half ranking one of the commercial mask sizes as most comfortable. Comfort rankings were poorly correlated with measured mask leak, likely indicating that subjects' perception of comfort was more strongly influenced by other factors, such as the pressure of the mask contacting the face or localized leaks directing airflow towards the eyes. While measurement of airflow from the CPAP machine allows the total mask leak to be derived, it provides no information on the location of the leak around the interface between the mask cushion and face. When evaluating customized masks for CPAP, Cheng *et al.* (Cheng *et al*., 2015) divided their comfort assessment into several components: headgear force, headgear comfort, cushion fit, cushion comfort, forehead comfort, and usability. Their study found better performance in headgear force and cushion fit for their customized masks, but found no significant correlation between headgear tightness or cushion fit with cushion comfort (Cheng *et al*., 2015). Overall, no statistically significant difference in cushion comfort was found between customized and commercial masks (Cheng *et al*., 2015).

Prevalence of OSA is higher in subjects with craniofacial abnormalities than in the general population (Tan *et al*., 2016), some of whom may not be able to maintain CPAP therapy using commercial masks. Morrison *et al.* (Morrison *et al*., 2015) developed a custom-built oronasal mask for a child with craniofacial abnormalities and OSA which decreased mask leakage, improved AHI, and increased adherence, which were all sustained after three months of use. Such benefits to patients present potential savings to healthcare systems, which may ultimately offset the fabrication costs of custom masks. Based on results from both our study and the study by Morrison *et al.* (Morrison *et al*., 2015), custom fabricated CPAP masks may be most suitable to a population with craniofacial abnormalities that are unable to use commercial masks. Further study of the custom-built nasal masks presented herein in subjects with craniofacial abnormalities is warranted.

2.5 Conclusion

Customized masks successfully delivered and maintained target CPAP settings in all six adult subjects, demonstrating the feasibility of the mask customization methods employed. Customized masks should be explored for individuals with unique facial features who are unable to receive CPAP treatment using commercial masks.

Chapter 3: Comparison of Airway Pressures and Gas Washout for Nasal High Flow versus CPAP in Child Airway Replicas

A version of this chapter will be submitted to a scientific journal for publication.

3.1 Introduction

Obstructive sleep apnea (OSA) is a common sleep-related breathing disorder in which an individual's upper airway is obstructed, causing partial to complete interruptions in their breathing. OSA affects both adults and children, but the consequences of the disorder may differ between the two groups. The negative impact OSA has on cognitive, learning, and behavioural functions are more serious in children than in adults (Alsubie and BaHammam, 2017; Bhattacharjee *et al*., 2009; Gozal and O'Brien, 2004). Other complications in children include cardiovascular complications and impacts on growth (Alsubie and BaHammam, 2017; Bhattacharjee *et al*., 2009; Ingram *et al*., 2017; Marcus, Greene, & Carroll, 1998). OSA is estimated to affect between 1 % to 10 % of children (Alsubie and BaHammam, 2017; Andersen, Holm, & Homøe, 2016; Chan, Edman, & Koltai, 2004; Marcus *et al*., 2012).

The delivery of continuous positive airway pressure (CPAP) is an effective treatment for OSA in children (Marcus *et al*., 2006; Sawyer *et al*., 2011). CPAP restores breathing and sleep by acting as a pneumatic stent to prevent the collapse of the upper airways. Typically, a nasal/facial mask, preferably selected to conform as best as possible to the individual's facial geometry, is used to administer CPAP (Strickland, 2019). Though effective, adherence to the therapy is poor due to discomfort (Salepci *et al*., 2013; Valentin *et al*., 2011). Multiple factors contribute to discomfort, such as mask leak, skin irritation, and/or pressure sores (Ahn, 2010; Bhattacharjee *et al*., 2020). With the goal of improving adherence to CPAP therapy, several

groups have investigated improvements to the comfort of the mask interface (Cheng *et al*., 2015; Duong *et al*., 2021; Sela *et al*., 2016; Shikama *et al*., 2018). However, other groups have explored alternative forms of non-invasive respiratory support, including administration of nasal high flow (NHF) therapy (Amaddeo *et al*., 2019; McGinley *et al*., 2009).

The delivery of NHF for OSA in children has been investigated as an alternative to mask-based CPAP (Amaddeo *et al*., 2019; Hawkins *et al*., 2017; McGinley *et al*., 2009). NHF therapy generates positive airway pressure through the delivery of humidified air or air/oxygen mixtures at high flow rates through nasal cannulas. In studies by Hawkins *et al.* (Hawkins *et al*., 2017) and Amaddeo *et al.* (Amaddeo *et al*., 2019), both groups assessed NHF therapy in children who were intolerant to CPAP therapy. NHF therapy was shown to have good compliance in children and was able to reduce respiratory events (Amaddeo *et al*., 2019; Hawkins *et al*., 2017). In addition to positive airway pressure, NHF therapy is known to provide washout of the nasopharyngeal dead space (Dysart *et al*., 2009). These benefits make NHF therapy a promising alternative for CPAP-intolerant children.

In the present work, upper airway pressures and carbon dioxide washout were compared between NHF and CPAP therapy *in vitro* using child airway replicas coupled to a lung simulator.

3.2 Methods

In this *in vitro* study, the delivery of NHF through nasal cannula was compared with the delivery of CPAP through a nasal mask. The study was conducted using the upper airway replicas of 10 child subjects, with two main comparative measurements: tracheal pressures and end-tidal carbon dioxide concentration (EtCO2). Tracheal pressures were separated into four parameters:

positive end-expiratory pressure (PEEP), peak pressure, minimum pressure, and average inspiratory pressure.

3.2.1 Child Airway Replicas

The 10 upper airway replicas, which include the nose-throat airway and terminate at the trachea, were previously fabricated in our research group based on computed tomography (CT) scan data of 10 child subjects, between the ages of 4 and 8 years, as reported by Paxman *et al.* (Paxman *et al*., 2019). The replicas were 3D printed (Objet Eden 350 V; Stratasys Ltd., MN, USA) using a rigid opaque photopolymer material (VeroGray; Stratasys Lt., MN, USA). Further details on the fabrication of the replicas can be found in the work by Paxman *et al* (Paxman *et al*., 2019). For the present study, branching airways downstream of the carina were removed from the replicas, and 3D printed adapters were attached to the exit of each replica to standard 22 mm breathing circuit tubing. Demographic data and geometric properties of the replicas are presented in Table 3.1.

Table 3.1: Mask air leak for each subject's preferred commercial CPAP mask and their customized counterparts at an appropriate fit (350 g). SLPM: standard litres per minute.

Subject Number	Age	Sex	Height (m)	Weight (kg)	Airway Volume (mL)	Area of Nostrils (mm^2)
2	5	M	1.17	22.9	40.4	55
3	5	M	1.12	20.0	35.1	115
5	6	F	1.12	18.0	19.1	85
6	6	F	1.18	21.5	32.1	66
9	5	M	1.13	20.0	21.0	80

10	4	F	0.99	16.0	19.2	58
11	8	M	1.25	24.5	48.4	100
12	6	F	1.24	24.0	22.2	86
13	7	F	1.21	20.0	32.5	84
14	4	F	1.00	16.0	18.6	56

3.2.2 Experimental Apparatus

A lung simulator (ASL 5000 Breathing Simulator; IngMar Medical, Pittsburgh, PA, USA) was used to simulate tidal breathing through the replicas.

For the present study, breathing frequency (f) and inspiratory/expiratory (i/e) ratio were fixed at 17 breaths per minute (BPM) and 0.85, respectively. Tidal volume (V_t) was fixed at 10 mL/kg body weight yielding a range of 160 to 245 mL. These breathing parameters were selected as typical in studies involving high flow and CPAP delivery to children in this age group (Baumert *et al*., 2016; Immanuel *et al*., 2012; Taussig, Harris, & Lebowitz, 1977). With these three parameters, the inspiratory and expiratory phases of a breath were modeled as half-sine waves with no inspiratory or expiratory pause.

For tracheal pressures, the intervention, either CPAP or NHF, was applied to the replica which was connected to the lung simulator through standard 22 mm breathing circuit tubing (Figure 3.1). The length of tubing was kept short to minimize pressure losses and measured 17.0 cm.

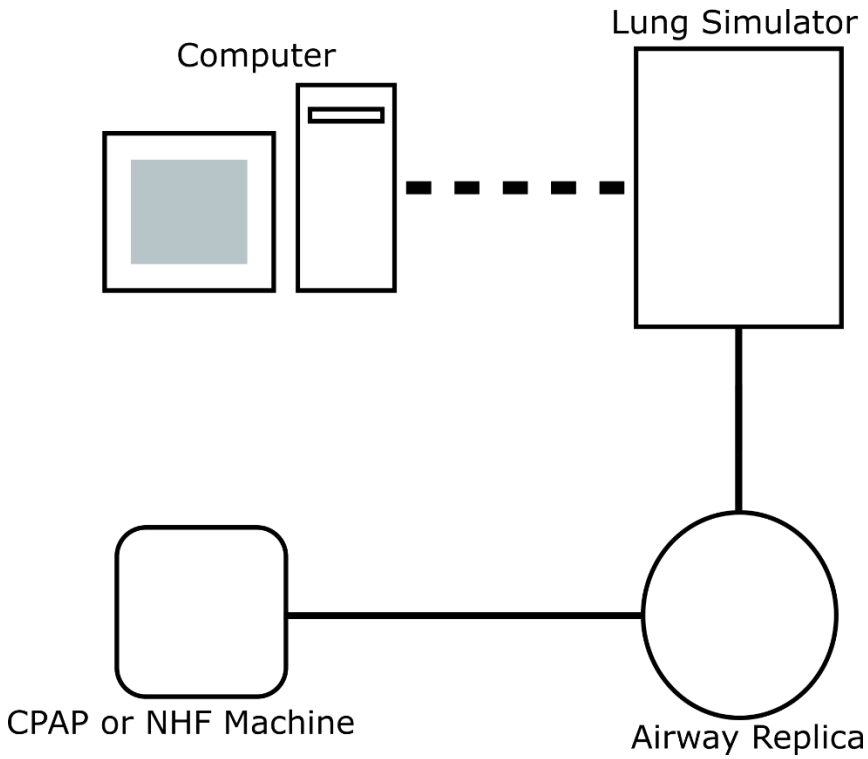

Figure 3.1: Schematic of experimental apparatus for measuring tracheal pressures

For $EtCO_2$, an intervention was applied to the replica, which was connected to the lung simulator through two airway adapters and a static mixer (Figure 3.2). A capnograph (EMMA Capnograph; Masimo, Irvine, CA) was attached to the adult/pediatric EMMA Airway Adapter (Masimo, Irvine, CA), positioned between the replica and mixer, to measure $EtCO_2$ through infrared spectroscopy. The resulting $EtCO_2$ was displayed as a running average on the screen of the capnograph in mmHg along with the respiratory rate. A straight connector with 7.6 mm port (1964000; Intersurgical, Wokingham, Berkshire, UK) was positioned between the mixer and lung simulator, and used for injection of CO_2. The mixer was used to ensure that the supplied CO_2 was well mixed in the breathing circuit before reaching the capnograph (Martin *et al*., 2016). The internal volume of the connection between the replica and the lung simulator measured 59.2 mL.

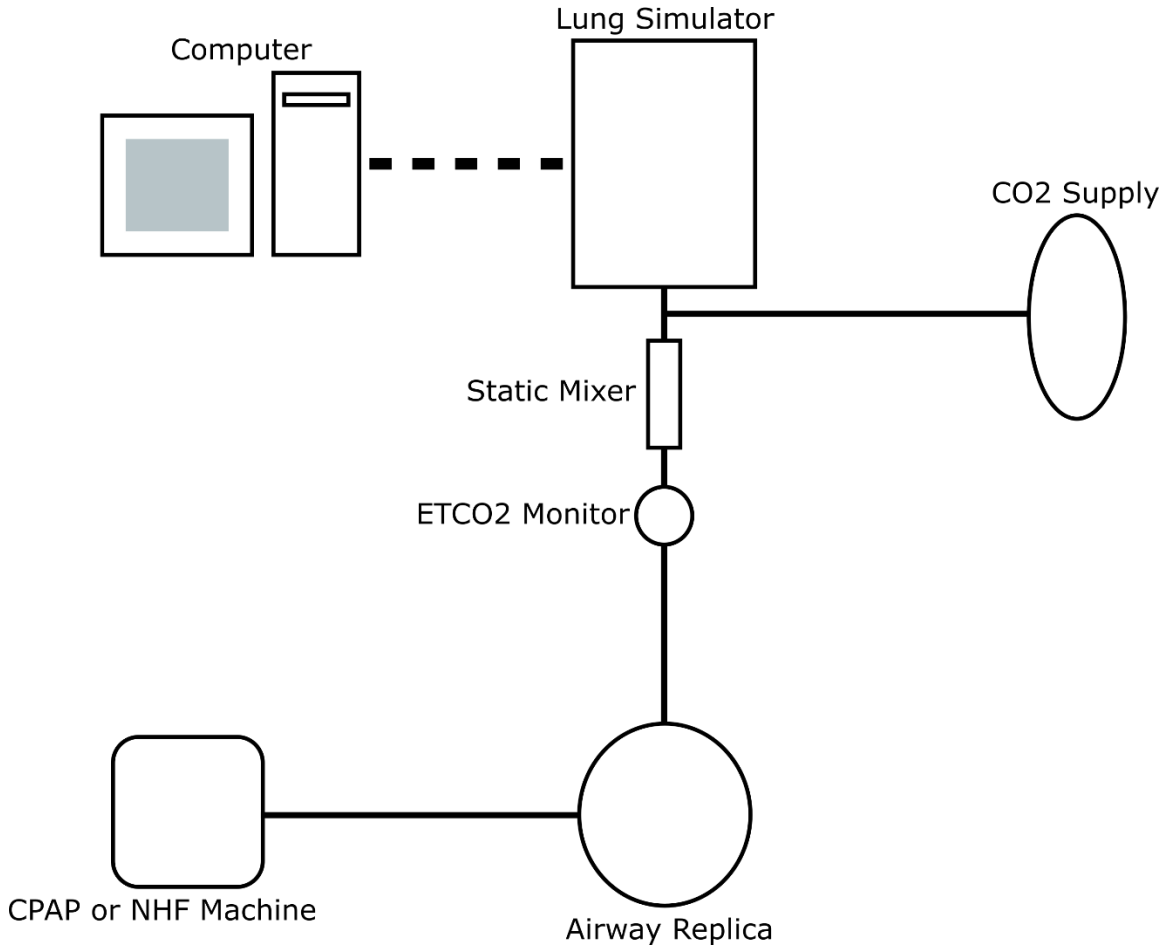

Figure 3.2: Schematic of experimental apparatus for measure EtCO2

A constant flow of 100 % CO_2 was bled inline to achieve 5% $EtCO_2$ as a baseline during simulated breathing through each replica without any intervention applied. $EtCO_2$ was converted from mmHg to % CO_2 at an average atmospheric pressure of 707.32 mmHg (Edmonton, Alberta, Canada) over the testing period of the experiments. The required CO_2 injection rates ranged from 60 mL/min to 130 mL/min depending on the replica, and are displayed in Table 3.2. $EtCO_2$ values measured during each tested intervention were reported as a change in % CO_2 from baseline.

Table 3.2: Tidal volume and CO_2 injection rates for each airway replica

Subject Number	Tidal Volume (mL)	CO_2 Injection Rate (mL/min)
2	229	115
3	200	95
5	180	80
6	215	100
9	200	95
10	160	60
11	245	130
12	240	130
13	200	85
14	160	60

3.2.3 Nasal High Flow

NHF was delivered with a humidified Nasal High Flow system, Airvo 2, which was provided by Fisher & Paykel Healthcare (Auckland, New Zealand). During the study, the supplied flow was set at a flow rate of 20 L/min, consistent with the flow rate used in studies by McGinley *et al.* and Amaddeo *et al.* that investigated NHF for treating OSA in children with a similar age range as the present study (Amaddeo *et al*., 2019; McGinley *et al*., 2009). Temperature was set at 34 °C with supplied oxygen concentration set at 21%. Three high flow nasal cannulas were tested, which were provided by Fisher & Paykel Healthcare: the Optiflow 3S Nasal Cannula (small, OPT1042), the Optiflow + Nasal Cannula (small, OPT942), and the Optiflow Junior 2 Nasal

Interface (XL, OJR418). The inner and outer diameters for each nasal cannula prong are provided in Table 3.3.

Table 3.3: Inner and outer diameters of nasal cannula prongs

	Diameter (mm)	
Nasal Cannula	Inner	Outer
Optiflow 3S	4.2	5.0
Optiflow +	4.1	4.9
Optiflow Junior 2	3.0	3.8

During administration of NHF, PEEP is generated in the upper airway as supplied flow from the cannula reverses direction and exits the airway around the obstruction created by the presence of the nasal prongs positioned in the nares. In fluid mechanics, pressure losses due to obstructions are commonly modeled as minor losses, and may be correlated with Reynolds number (Re) (Çengel and Cimbala 2006). Therefore, the correlation between a minor loss coefficient (K) associated with PEEP and Reynolds number was evaluated. Re was calculated using the characteristic air speed through the non-occluded nares area (U), determined by the flow rate (Q) divided by the area between the nostril walls and the outer wall of the cannula prongs ($A_{non\text{-}occluded}$):

$$U = \frac{Q}{A_{non\text{-}occluded}} \quad (1)$$

The hydraulic diameter (D_h) was calculated by treating the area between the nostril walls and the outer wall of the cannula prongs as an annular cross-section:

$$D_h = D_{OD} - D_{ID} \quad (2)$$

where the inner diameter of the nostril wall is D_{OD} and the outer diameter of the prong is D_{ID}. With these definitions of U and D_h, Re was:

$$Re = \frac{\rho U D_h}{\mu} \quad (3)$$

where density of air (ρ) at 34 °C was 1.15 kg/m^3 and dynamic viscosity (μ) was 1.89E-5 kg/m*s.

A minor loss coefficient associated with PEEP was then calculated as:

$$K = \frac{2(\text{PEEP})}{\rho U^2} \quad (4)$$

3.2.4 Continuous Positive Airway Pressure

CPAP was delivered using a CPAP machine (S8 Elite; ResMed, San Diego, CA, USA) connected to a nasal mask (Infant Pocket Mask; nSpire Health Inc., CO, USA) through supply tubing including an exhalation port (Wisp tube and elbow assembly; Philips Respironics, Murrysville, PA, USA). Masks were sealed to the face of each child replica using silicone adhesive. A Pitot tube flow sensor (RespEQ, Baltimore, MD, USA) (Kirkness *et al*., 2011) was attached inline between the CPAP machine and the mask to measure the air flow in real time in standard litres per minute (SLPM; with standard conditions defined as 21.1 ºC and 101.3 kPa). SLPM was converted to L/min during analysis using average conditions of the lab during the testing period (21.1 ºC and 94.3 kPa; Edmonton, Alberta, Canada). The flow waveform was used to calculate the leak flow through the exhalation port, averaged over the breathing cycle, and to

ensure that unintended mask leak was at a minimum. This mask leak measurement system was validated and used in a previous study by Duong *et al.* (Duong *et al*., 2021). Two CPAP settings were selected for testing: 5 cmH_2O and 10 cmH_2O. These settings coincide with typical settings used for children of this age range (McGinley *et al*., 2009).

As a preliminary experiment, we compared the tracheal pressures between CPAP for minimal mask leak and for a leak introduced near the mask (~14 L/min for 5 cmH_2O and ~20 L/min for 10 cmH_2O). This was done for subjects 2, 9, 10, and 13. The resulting tracheal pressures of the subjects under the leak were similar to those found under minimal leak. Based on these results, we determined that conducting further experiments with a mask leak was not warranted. All results presented below were obtained with the mask sealed to the face of each airway replica.

3.2.5 Study Design

The study was done in two parts, one for assessing tracheal pressures and one for assessing $EtCO_2$.

For tracheal pressures, CPAP settings of 5 and 10 cm H_2O were tested for all 10 replicas. For NHF, the Optiflow Junior 2 nasal cannula was tested in all 10 replicas, but the Optiflow 3S and Optiflow + nasal cannulas were only tested in five replicas (subjects 3, 5, 11, 12, and 13), as prong sizes were too large to fit the nostrils of the other five replicas. A single test ran for approximately 30 breaths while tracheal pressures were recorded by the lung simulator. The pressures were each averaged over five breaths, breaths 21 – 25, and were used for further analysis. Each intervention was tested three times for each replica, and the NHF cannula prongs were repositioned between repetitions.

For $EtCO_2$, three CPAP settings were tested for all 10 replicas: 5 cmH_2O, 10 cmH_2O, and zero CPAP (with the sealed mask in place). For NHF, similar to the pressure tests, the Optiflow Junior 2 was tested for all 10 replicas, but the Optiflow 3S and Optiflow + were tested for five replicas. A single test ran until $EtCO_2$ reached steady state and was recorded, typically taking ~80 to 100 breaths. Again, each intervention was tested three times for each replica, and the NHF cannula prongs were repositioned between repetitions.

3.2.6 Statistical Analysis

A set of one factor repeated measures Analysis of Variance (ANOVA) procedures were done along with Tukey post hoc analysis comparing the tracheal pressures and change in $EtCO_2$ between CPAP and NHF (n = 10). Three interventions were compared for the four tracheal pressure parameters: 5 cmH_2O CPAP, 10 cmH_2O CPAP, and the Optiflow Junior 2. Four interventions were compared for change in $EtCO_2$: zero CPAP (sealed mask), 5 cmH_2O CPAP, 10 cmH_2O CPAP, and the Optiflow Junior 2. Results with two-sided $P \leq 0.05$ was considered significant.

Another set of one factor repeated measures Analysis of Variance (ANOVA) procedures were done along with Tukey post hoc analysis comparing the tracheal pressures and change in $EtCO_2$ between the three NHF cannulas (n = 5). Three interventions were compared for the four tracheal pressure parameters and change in $EtCO_2$: the Optiflow 3S, the Optiflow +, and the Optiflow Junior 2. Results with two-sided $P \leq 0.05$ was considered significant. Statistical analysis was performed with MATLAB (MathWorks, Natick, MA, USA).

3.3 Results

3.3.1 Comparison of CPAP vs NHF

The delivered flow rate of air during CPAP, averaged over the breath, was measured as 18.8 ± 1.1 L/min for 5 cmH_2O and 26.1 ± 1.6 L/min for 10 cmH_2O (mean ± standard deviation; n = 10 replicas).

Average PEEP, peak pressure, minimum pressure, and inspiratory pressure across the 10 replicas for the three intervention types are displayed in Figure 3.3. From ANOVA, the selection between CPAP and NHF was observed to have a significant influence on tracheal pressures. From post hoc analysis, 5 cmH_2O CPAP was different from 10 cmH_2O CPAP for all four pressure parameters, but different from NHF only in terms of peak and minimum pressures. 10 cmH_2O CPAP was different from NHF in terms of PEEP, minimum pressure, and average inspiratory pressure. Sample pressure waveforms for all individual replicas during administration of CPAP and NHF are displayed in Figure 3.4.

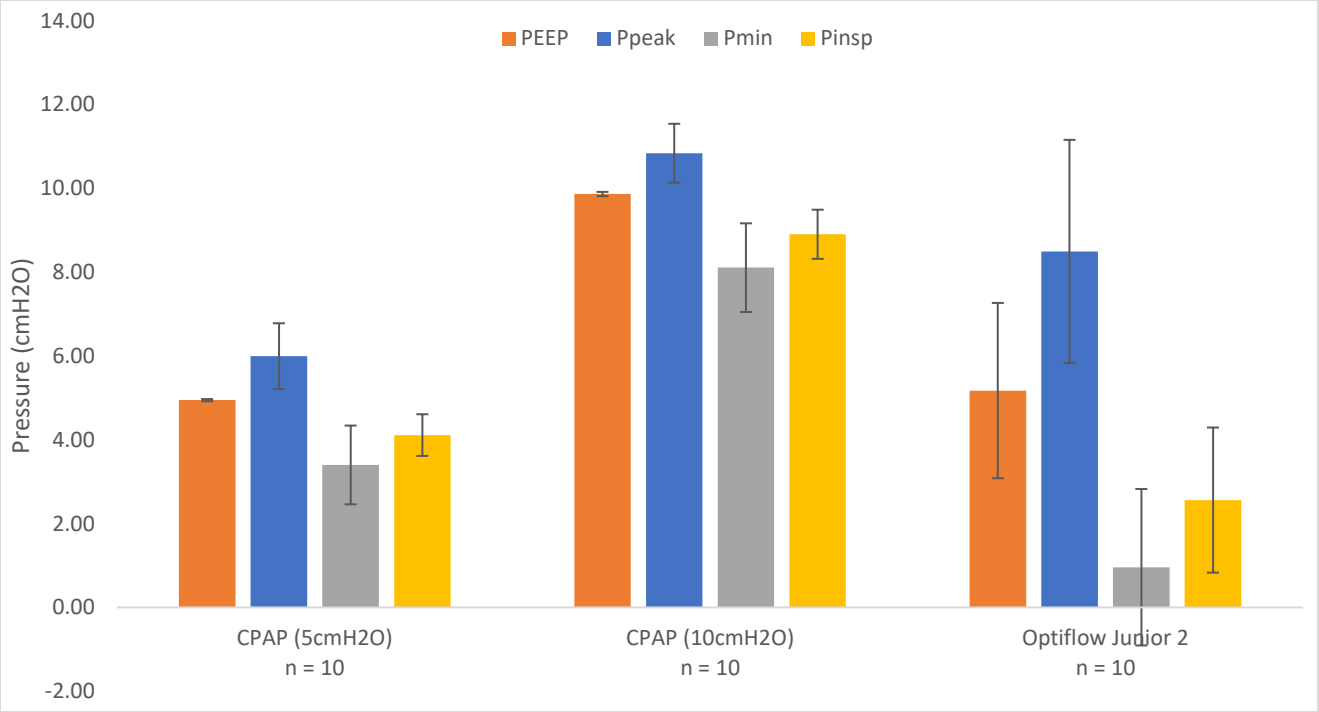

Figure 3.3: Average tracheal pressures across all 10 airway replicas for CPAP at 5cmH_2O, CPAP at 10cmH_2O, and NHF with the Optiflow Junior 2 cannula. Error bars represent one standard deviation around the average. PEEP = positive end-expiratory pressure. Ppeak = peak pressure. Pmin = minimum pressure. Pinsp = average inspiratory pressure

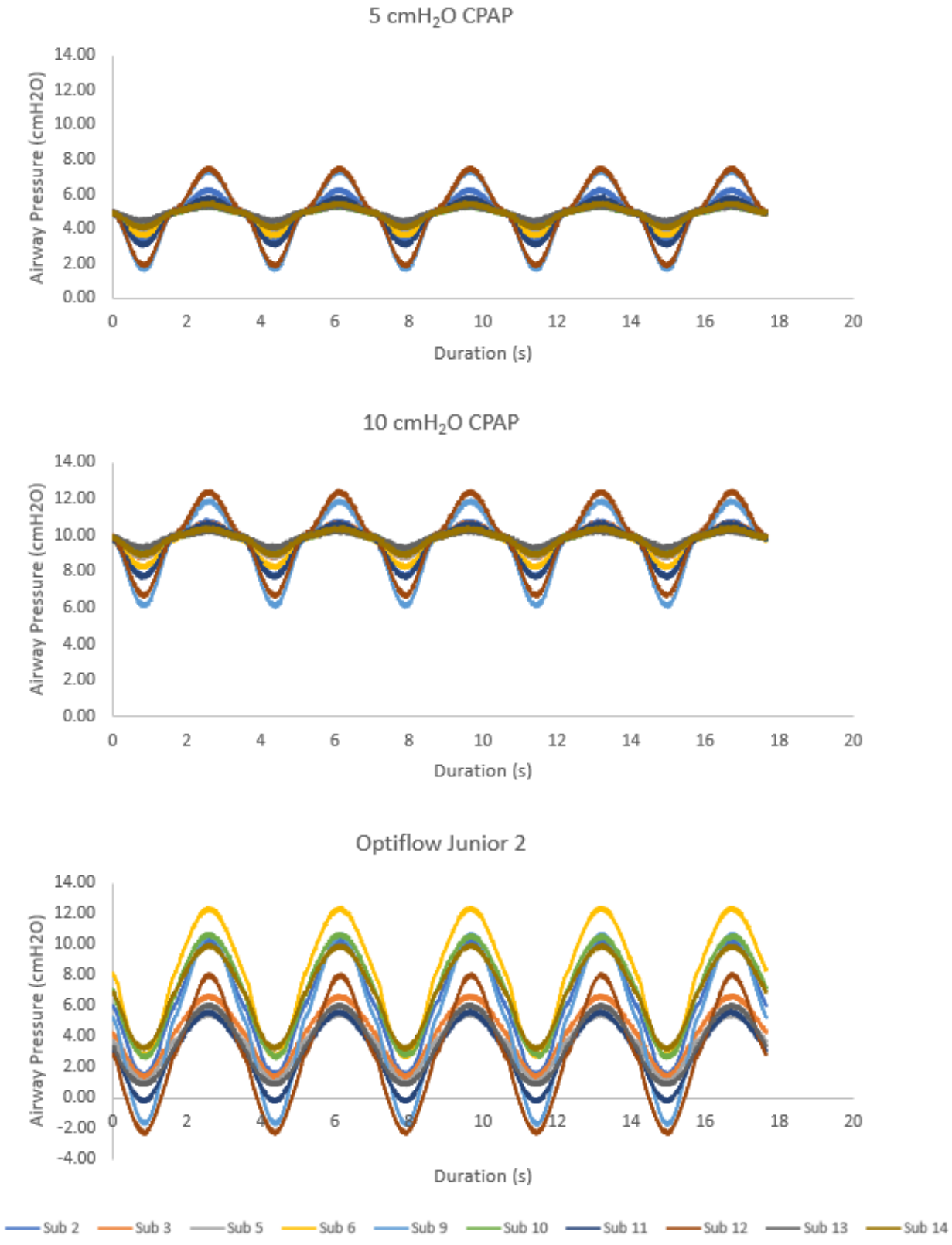
5 cmH2O CPAP
Airway Pressure (cmH2O)
14.00
12.00
10.00
8.00
6.00
4.00
2.00
0.00
0
2
4
6
8
10
12
14
16
18
20
Duration (s)
10 cmH2O CPAP
Airway Pressure (cmH2O)
Duration (s)
Optiflow Junior 2
Airway Pressure (cmH2O)
-2.00
-4.00
Duration (s)
Sub 2
Sub 3
Sub 5
Sub 6
Sub 9
Sub 10
Sub 11
Sub 12
Sub 13
Sub 14

Figure 3.4: Tracheal pressure waveforms measured over 5 breaths during administration of 5 cmH_2O CPAP (top), 10 cmH_2O CPAP (middle), and NHF using the Optiflow Junior 2 cannula (bottom).

Average change in $EtCO_2$ from baseline across the 10 replicas for the four intervention types are displayed in Figure 3.5. Selection between CPAP and NHF was observed to have a significant influence on change in $EtCO_2$. From post hoc analysis, all interventions tested were different from one another in terms of average change in $EtCO_2$, except for the pairing of zero CPAP (with the sealed mask in place) and 5 cmH_2O CPAP.

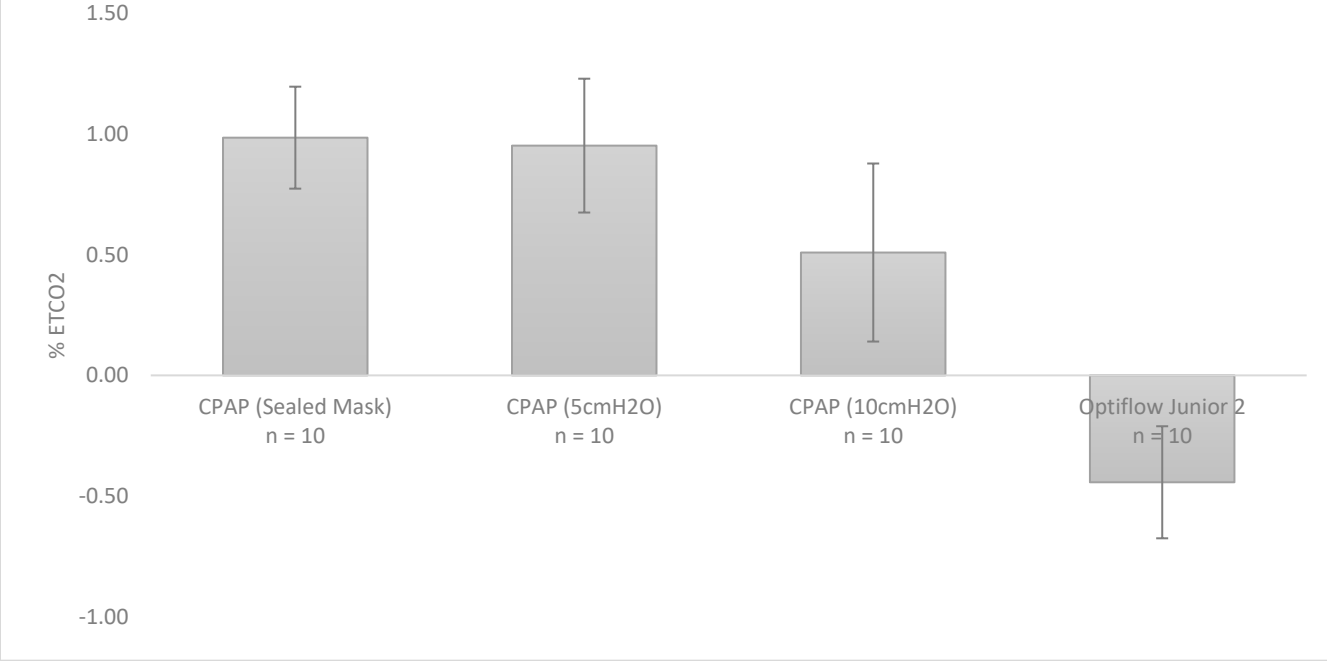

Figure 3.5: Average change in $EtCO_2$ from baseline across all 10 airway replicas for CPAP with sealed mask on (but zero CPAP applied), CPAP at 5cmH_2O, CPAP at 10cmH_2O, and NHF with Optiflow Junior 2. Error bars represent one standard deviation around the average.

3.3.2 Comparison Between Three NHF Cannulas

Average PEEP, peak pressure, minimum pressure, and inspiratory pressure across the five replicas tested with three different NHF cannulas are displayed in Figure 3.6. From ANOVA, the selection of nasal cannula was not observed to have a statistically significant influence on tracheal pressures. Sample pressure waveforms for the five tested replicas during administration of NHF for all three nasal cannulas are displayed in Figure 3.7.

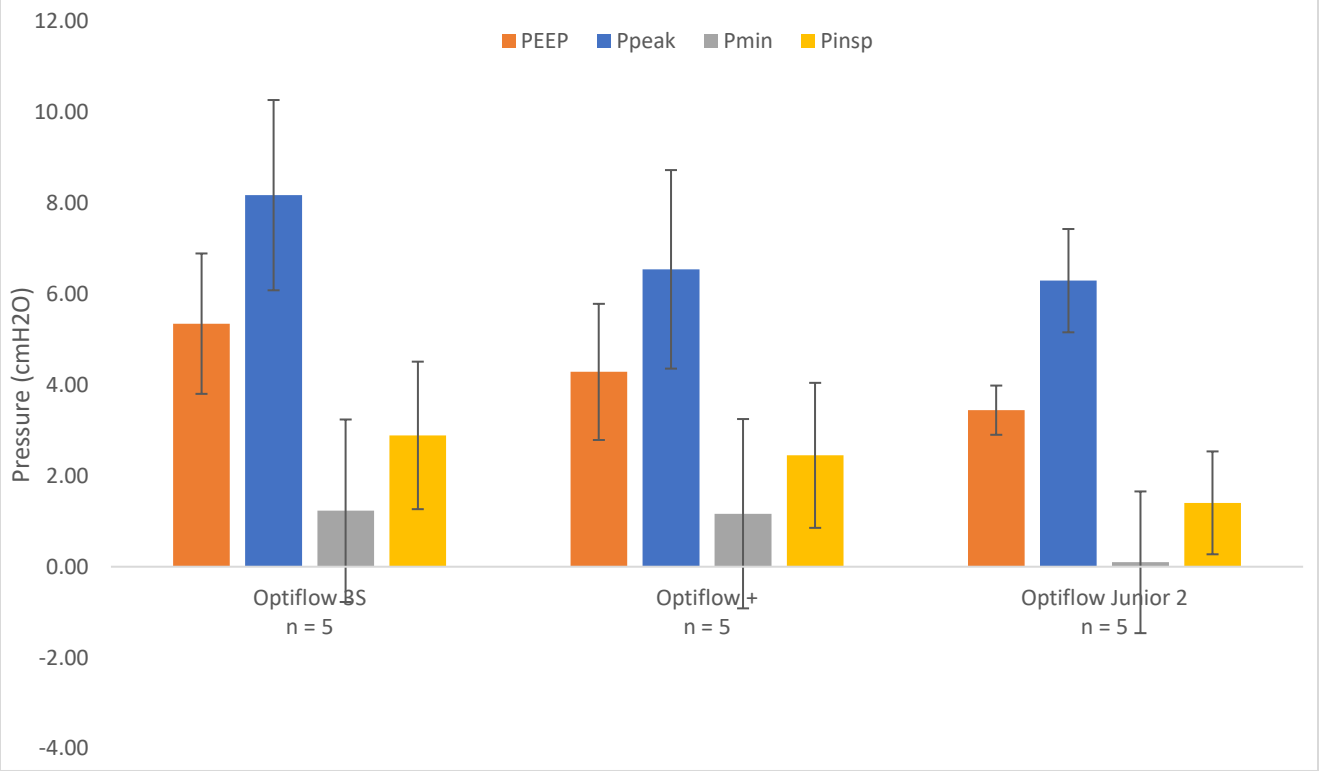

Figure 3.6: Average tracheal pressures across 5 airway replicas for three NHF cannulas, Optiflow 3S, Optiflow +, and Optiflow Junior 2. Error bars represent one standard deviation around the average. PEEP = positive end-expiratory pressure. Ppeak = peak pressure. Pmin = minimum pressure. Pinsp = average inspiratory pressure

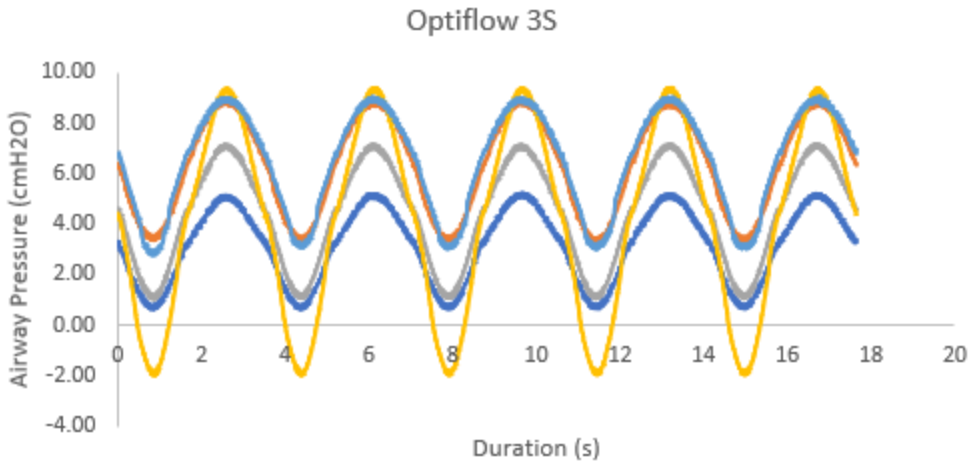
Optiflow 3S
Airway Pressure (cmH2O)
10.00
8.00
6.00
4.00
2.00
0.00
-2.00
-4.00
0
2
4
6
8
10
12
14
16
18
20
Duration (s)

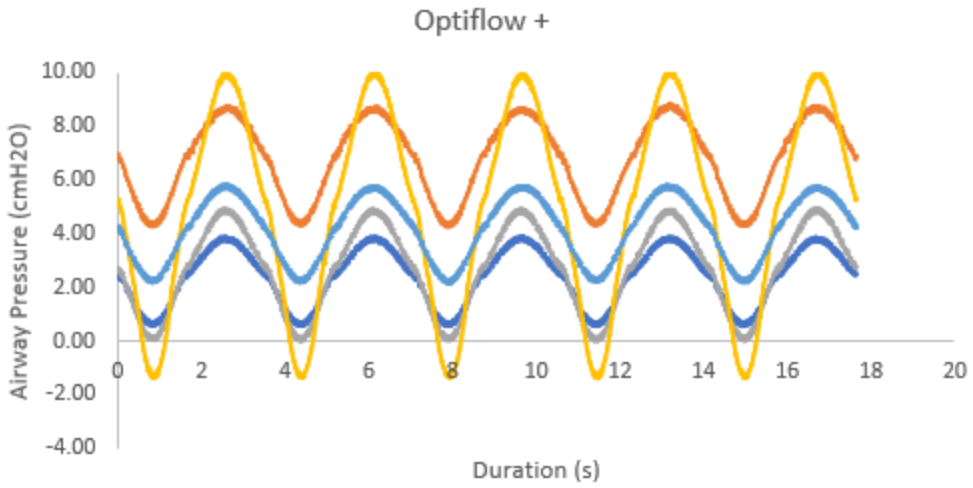
Optiflow +
Airway Pressure (cmH2O)
10.00
8.00
6.00
4.00
2.00
0.00
-2.00
-4.00
0
2
4
6
8
10
12
14
16
18
20
Duration (s)

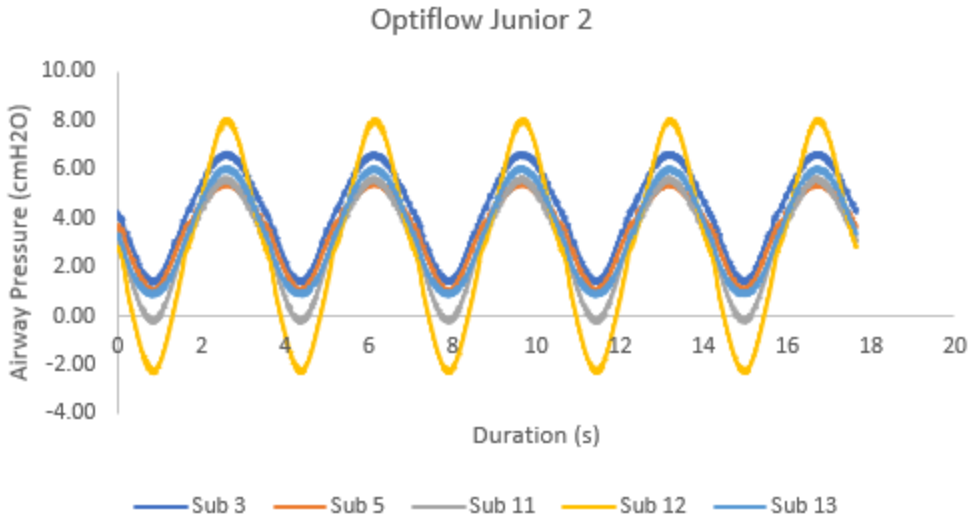
Optiflow Junior 2
Airway Pressure (cmH2O)
10.00
8.00
6.00
4.00
2.00
0.00
-2.00
-4.00
0
2
4
6
8
10
12
14
16
18
20
Duration (s)
Sub 3
Sub 5
Sub 11
Sub 12
Sub 13

Figure 3.7: Tracheal pressure waveforms measured over 5 breaths during administration of NHF using the Optiflow 3S cannula (top), the Optiflow + cannula (middle), and the Optiflow Junior 2 cannula (bottom).

Average change in $EtCO_2$ from baseline across the five tested replicas for NHF are displayed in Figure 3.8. Similar to tracheal pressures, selection of nasal cannula was not observed to have a statistically significant influence on change in $EtCO_2$.

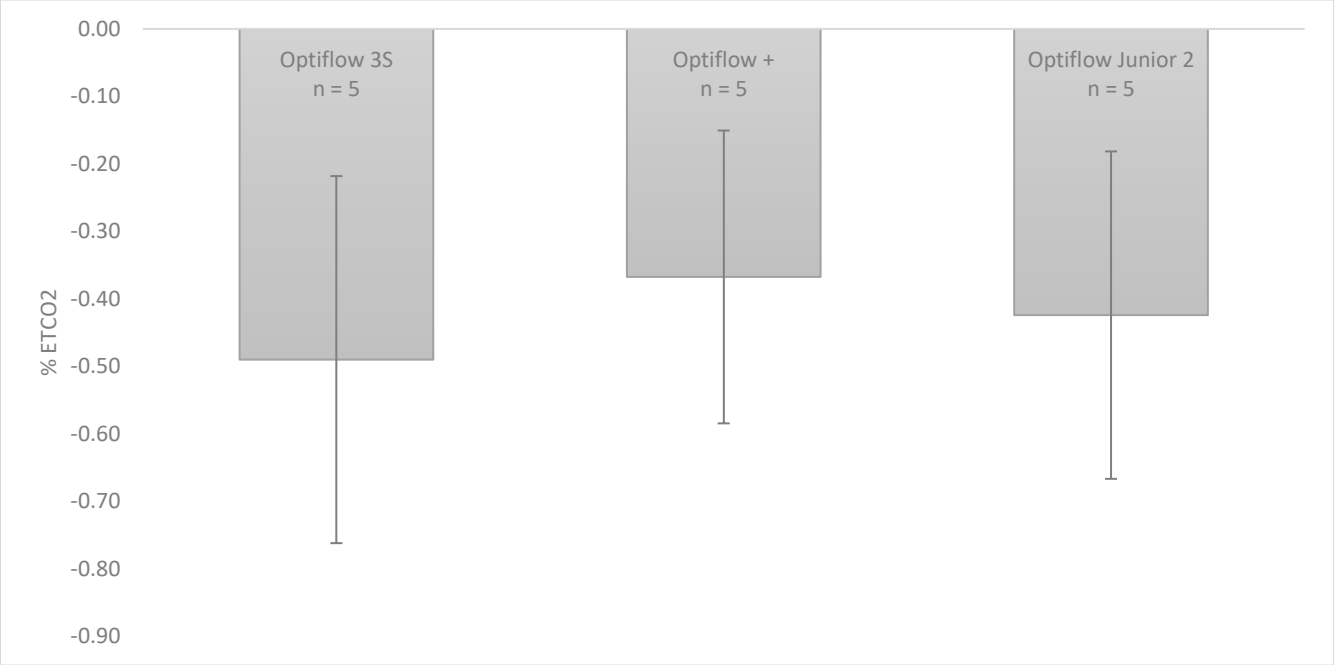

Figure 3.8: Average change in $EtCO_2$ from baseline across 5 airway replicas for the three NHF cannulas. Error bars represent one standard deviation around the average.

3.3.3. Minor Loss Coefficients and Reynolds Numbers

Across the three NHF cannulas and ten replicas, the Reynolds numbers calculated using Equation 3 ranged from 950 – 1350. Minor loss coefficients calculated using Equation 4 for the Optiflow 3S and Optiflow + cannulas, and averaged over five replicas, were 23 ± 4 and 20 ± 5,

respectively (average ± standard deviation). The minor loss coefficient for the Optiflow Junior 2 cannula, averaged over the larger set of ten replicas, was 23 ± 13.

3.4 Discussion

Results of *in vitro* experiments evaluating tracheal pressures and $EtCO_2$ during delivery of CPAP or NHF to child airway replicas are reported above. Several differences between CPAP and NHF warrant further discussion, as do the potential sources of variability in pressure and gas washout between airway replicas.

For the delivery of CPAP, PEEP was observed to be approximately constant across the 10 airway replicas at either 5 cmH_2O or 10 cmH_2O (Figure 3.3), indicating that the CPAP machine was working as intended, and delivered targeted positive airway pressures. In contrast, peak pressure, minimum pressure, and average inspiratory pressure were observed to vary between replicas, indicating that these three pressure parameters were influenced by additional factors including breathing flow rates and the airway geometries of each subject (Figure 3.4). This was expected, as airway pressure was evaluated at the exit of each replica (representative of a tracheal pressure), such that pressure drop through the replica influenced the airway pressure in all cases where flow was nonzero. In contrast, PEEP was measured at a point on the breathing cycle of zero flow, such that the instantaneous pressure drop through the replica is also zero.

Unlike the CPAP machine, the NHF system does not adjust delivered flow rate to maintain a constant pressure. As such, all pressure parameters, including PEEP, were observed to be variable across the 10 airway replicas for the delivery of NHF (Figures 3.3 and 3.4). With a set flow rate of 20 L/min, the average PEEP across the 10 airway replicas was approximately 5

cmH_2O, which is similar to a CPAP setting of 5 cmH_2O. Accordingly, though NHF can generate positive airway pressures, the pressures are variable and subject-dependent. McGinley *et al.* (McGinley *et al*., 2009) reported on the delivery of NHF as an alterative to CPAP for children aged 10 ± 1 years (mean ± SEM; n = 12) at a set flow rate of 20 L/min. In their study, they found similar reductions in apnea-hypopnea index, comparable to CPAP prior to the study, when using NHF in a majority of the children studied (McGinley *et al*., 2009). Prior to NHF, the average CPAP setting used for therapy was 9 ± 1 cmH_2O (mean ± SEM; n = 10) (McGinley *et al*., 2009).

An increase in $EtCO_2$ from baseline was observed during CPAP therapy across all 10 upper airway replicas. The presence of a mask increased $EtCO_2$, due to added dead space of the mask. This increase was smallest for CPAP at 10 cmH_2O (Figure 3.5), owing to the greater average flow rate delivered from the CPAP machine at the higher CPAP setting. In contrast, a reduction in $EtCO_2$ from baseline was observed during NHF therapy across all 10 upper airway replicas. This is consistent with a known mechanism of NHF: washout of the nasopharyngeal dead space, leading to reduced rebreathing of expired air (Dysart *et al*., 2009; Möller *et al*., 2017). It is notable that, due to differences between the NHF cannula interface and CPAP mask interface, effective washout was observed for NHF at a flow rate of 20 L/min, whereas no, or limited, washout was observed for CPAP with an average delivered flow rate of 18.8 L/min (for CPAP at 5 cmH_2O), or 26.1 L/min (10 cmH_2O).

No significant difference was observed in tracheal pressures nor change in $EtCO_2$ between the three different NHF cannulas for the subset of five tested replicas. An average PEEP of 5.4 ± 1.6 cmH_2O, 4.3 ± 1.5 cmH_2O, and 3.5 ± 0.5 cmH_2O were generated through the Optiflow 3S, +, and Junior 2 nasal cannula, respectively (Figure 3.6). Though not statistically significant, differences in average PEEP between cannula models may be associated with

different cannula prong sizes, as has been noted to influence PEEP in previous studies (Moore *et al*., 2020; Moore *et al*., 2019). All three nasal cannulas also had similar reductions in $EtCO_2$ from baseline: -0.5 ± 0.3 % for the Optiflow 3S, -0.4 ± 0.2 % for the Optiflow +, and -0.4 ± 0.2 % for the Optiflow Junior 2 (Figure 3.8). However, only five replicas were tested because two of the three nasal cannula models, the Optiflow 3S and the Optiflow +, did not fit the five remaining replicas. This indicates that the selection of nasal cannula for NHF is important for fit and proper delivery of therapy. Relationships between reduction in $EtCO_2$ from baseline with tidal volume and replica volume were also investigated; however, no correlation was observed (Appendix: Figures A3 and A4). It may be that variability in gas washout during NHF was influenced by the shape of the replica airways, especially the nasal vestibule in immediate proximity of cannula prongs; however, this was not investigated in detail in the present study.

The increased variability between replicas in tracheal pressures generated during NHF as compared to CPAP is noticeable in Figures 3.3 and 3.4. Variability in PEEP between replicas was accounted for in part by modeling the pressure drop through the annular space between the prongs and nostril walls as a minor loss. Such a model is frequently adopted in fluid mechanics to calculate the pressure drop associated with flow through a constriction or past an obstruction. On average, calculated minor loss coefficients did not vary appreciably between the three NHF cannulas studied. Furthermore, minor loss coefficients remained approximately constant across the range of Reynolds numbers studied (Re = 950 to 1350), as is typically observed for flow through a constriction (Çengel and Cimbala 2006). Similarly, Katz et al. (Katz *et al*., 2011) previously adopted a minor loss model for the pressure drop through extrathoracic and bronchial airways, and observed that minor loss coefficients approach constant values as Reynolds numbers exceeded ~1000. In the present work, this relationship suggests that PEEP generated in

the replicas by NHF was related primarily to the occlusion of the nares by the cannula prongs. For a fixed flow rate of gas supplied to the cannula, the greater the extent of occlusion, the larger the PEEP that will be generated (Pinkham and Tatkov, 2020).

Some variability in calculated minor loss coefficients persisted between replicas, and can be attributed primarily to the dissimilar shape of the annular space for different replicas, which is not fully accounted for in the use of a single length scale, namely the hydrodynamic diameter calculated in Equation 2. Variation in the percentage of the nostrils' inlet area occluded by cannula prongs may also have contributed to variability between replicas in the minor loss coefficients. The greater variability in minor loss coefficient between replicas for the Optiflow Junior 2 cannula, as compared with the other two NHF cannulas studied, likely resulted from the larger number of replicas investigated with this cannula. For the subset of five replicas tested with all three NHF cannulas, the percent of occlusion ranged from 34 to 47 % for the Optiflow 3S, 33 to 45 % for the Optiflow +, and 20 to 27 % for the Optiflow Junior 2. When tested over the larger set of 10 replicas, the percent of occlusion ranged from 20 to 41 % for the Optiflow Junior 2.

Previously, Moore *et al.* (Moore *et al*., 2020; Moore *et al*., 2019) identified predictive correlations for PEEP generated during application of NHF based on a characteristic air speed through the non-occluded nares area, as in Equation 1 of the present study, but also on an additional characteristic air speed exiting the cannula prongs. In the present work, consideration of this additional characteristic air speed did not further improve our ability to account for variability in PEEP between nasal cannulas. This may in part be due to the limited range of air speeds exiting cannula prongs in the present study, which was conducted with a single flow rate supplied to nasal cannula. Furthermore, the Moore *et al.* studies included high flow nasal cannula

from a different manufacturer, which are intentionally designed with smaller inner diameters to influence washout of the upper airway (Miller, Saberi, & Saberi, 2016).

A limitation of this study is the use of rigid airway replicas. They did not deform during breathing or under positive airway pressures, and thus the dynamic effects of breathing are not fully captured. We tried to minimize this limitation by testing multiple airway replicas to cover a range of differing airway geometries. Variation in, e.g., airway volume or cross-sectional areas between different airway replicas is expected to be much greater than variation that occurs dynamically over an individual's breathing cycle. A second limitation is the testing of only one flow rate setting for NHF, 20 L/min, for our airway replicas with a subject age range of 4 – 8 years old. Previous studies have shown both airway pressures and washout to be flow rate dependent (Moore *et al*., 2020; Sivieri, Foglia, & Abbasi, 2017). However, clinical studies by McGinley *et al.* and Amaddeo *et al.* both used 20 L/min when investigating the use of NHF therapy as a treatment for OSA in children, aged 10 ± 1 years and 8.9 ± 6.2 years respectively (Amaddeo *et al*., 2019; McGinley *et al*., 2009). In both studies, NHF therapy at 20 L/min had a positive effect in treating OSA (Amaddeo *et al*., 2019; McGinley *et al*., 2009). Therefore, we focused on NHF at 20 L/min as a clinically-relevant flow rate for children with OSA.

3.5 Conclusions

NHF delivered at 20 L/min to child airway replicas generated average PEEP similar to CPAP at 5 cmH_2O. Variation in PEEP, and in the maximum and minimum airway pressures recorded over the breathing cycle, was greater between airway replicas for NHF than for CPAP. Application of NHF reduced $EtCO_2$ from baseline values, whereas delivery of CPAP through a sealed nasal mask increased $EtCO_2$ from baseline values. NHF may benefit children who are

non-compliant to CPAP therapy. Thus, further studies investigating NHF therapy as an alternative to CPAP therapy for treating OSA are warranted. These studies should consider potential beneficial effects of improved gas washout when administering NHF distinctly from the use of NHF to produce positive airway pressure.

Chapter 4: Conclusion

4.1 Summary

The focus of this thesis was to lend greater insight into alternatives and improvements to current OSA treatments. The current treatment relieves OSA-related consequences by delivering CPAP through a non-invasive mask tightened with a headgear. However, this method of delivery can cause significant discomfort for some, leading to concerns over insufficient adherence to the therapy. Alternative approaches may help improve comfort and thus adherence, as well as provide a treatment option for those who struggle or are unable to use commercially available masks.

The first alternative to be examined were customized nasal masks manufactured at the Live Cell Imaging Laboratory at the University of Calgary using 3D facial scanning and modern additive processes. A feasibility study was done comparing mask leakage and comfort between the customized nasal masks and commercially available ones in six healthy adult volunteers. Three CPAP levels were tested (4 cmH_2O, 8 cmH_2O, and 12 cmH_2O) to capture a range of settings typically used in adult patients. As expected, CPAP levels showed a direct relationship with mask leakage. Similarly, mask tightness (loose, appropriate, and tight) showed an inverse relationship with mask leakage. Three different commercial mask sizes—petite, small/medium, and large—were also tested to provide a range of fit from poor to good. The petite mask was unanimously found least comfortable, most likely since it was intended for pediatric use. The comfort of the other two commercial mask sizes and of the customized masks varied between the subjects, with half preferring the customized mask and half preferring a commercial size. For a loose fit, many mask and CPAP level combinations were unable to maintain their target settings,

as indicated by the "high leak" alarm from the CPAP machine. For the other two fits, the target CPAP settings were maintained for all combinations across all six subjects except for one subject using the petite mask at 12 cmH_2O with an appropriate fit. These results demonstrate that the customized nasal masks were able to deliver CPAP safely and effectively. The variability in mask leakage between subjects also appeared noticeably lower with the customized masks when they were compared to each subject's preferred commercial mask. However, a decrease in mask leakage was not consistently observed with the customized masks. There was high subject variability in relative mask leakage and comfort between the customized and preferred commercial masks, probably because of variable facial structures. The customized masks used in this study were not found to provide benefits to a general population with normal facial structures, but they may prove beneficial to a population with craniofacial abnormalities.

The second alternative examined was NHF therapy delivered through nasal cannulas. A pediatric population was the focus of this second investigation. A lung simulator was used both to simulate tidal breathing (17 bpm, 0.85 inspiratory/expiratory ratio, and 10 mL/kg body weight tidal volume) and to measure tracheal pressures in upper airway replicas drawn from 10 children aged 4 to 8 years. An average PEEP of ~ 5 cmH_2O and ~ 10 cmH_2O was measured across all replicas for a setting of 5 cmH_2O and 10 cmH_2O respectively; these were selected as the lower and upper ranges of the CPAP settings used for the target age group. This indicates that the CPAP machine was working as intended, being able to adjust its flow rate to maintain target CPAP levels. On the other hand, PEEP generated by NHF (set at 20 L/min) ranged from 3.5 to 5.4 cmH_2O depending on the nasal cannula selected. Unlike the CPAP machine, the NHF system does not have a way to adjust its flow rate. Though not statistically proven to make a difference, selection of cannula could nevertheless influence the positive airway pressures generated by

NHF. This study demonstrates that NHF set at 20 L/min can generate positive airway pressures similar to 5 cmH_2O CPAP and can thus be used as an alternative for those requiring a lower CPAP setting. The recorded peak pressures, minimum pressures, and average inspiratory pressures varied across the replicas, with a greater variation for NHF than for CPAP, suggesting that the former was more strongly influenced by airway geometries and tidal volumes. Washout of the nasopharyngeal dead space is a known mechanism of NHF therapy. For this reason, $EtCO_2$ was measured using a capnograph in both CPAP and NHF to compare the effects. As expected, a similar decrease in $EtCO_2$ from the baseline was seen across all replicas for NHF therapy through all three tested nasal cannulas. By contrast, CPAP, with an average flow rate of 18.8 L/min for 5 cmH_2O and 26.1 L/min for 10 cmH_2O, was observed to increase $EtCO_2$ from baseline values across all replicas. This suggests that the difference in interface—sealed nasal mask vs nasal cannula—could be the reason for the increase in $EtCO_2$ from the baseline for CPAP compared to NHF. NHF therapy can generate positive airway pressures similar to lower end CPAP settings used in a pediatric population and carries the additional benefit of dead space washout.

The research presented in this thesis lends valuable insight into the potential benefits of alternatives and improvements to current OSA treatments. Customized nasal masks investigated were able to deliver and maintain target CPAP settings. Though they were not found to benefit a general population, they might be beneficial to those with craniofacial abnormalities. Positive airway pressures similar to those of lower-end CPAP were generated by NHF therapy, with the added benefit of improved gas washout. Application of NHF could be beneficial for children who are intolerant of standard CPAP therapy. The results presented are intended to benefit other researchers looking into improving adherence to OSA treatments through alternative methods.

4.2 Future Work

The results presented in this thesis have shown that alternatives and improvements to current CPAP treatment for OSA could be beneficial and that further investigations are warranted. Regarding the customized nasal masks, these have been shown to effectively deliver target CPAP settings but did not appear any more beneficial for the general population than commercially available masks. However, they may be more favourable for a population with unique craniofacial features, especially children, in keeping with results found by Morrison *et al* (Morrison *et al*., 2015). A preliminary study to investigate the benefits of customized nasal masks in children who are having difficulties with their current CPAP masks is being planned. Using the same 3D facial scanning and additive processes, a customized nasal mask will be manufactured for each patient. The customized masks will go through a leak test using the flow sensor system described in Chapter 2 during each child's initial visit to ensure a good fit. Afterwards, the customized nasal masks will be compared to each patient's current mask through two at-home trials, one for each mask. AHI, mask leakage, and usage rate (hours/night for duration of study) will be measured using the data logged in the CPAP machines. These three metrics will be evaluated to determine the potential effectiveness of customized nasal masks for children with craniofacial abnormalities.

The NHF *in vitro* study demonstrated that for a flow rate of 20 L/min, approximately 5 cmH_2O airway pressure was generated in the upper airway replicas of children aged 4 to 8 years. Further investigations correlating other flow rates to generated positive airway pressures in this age group are therefore warranted. In undertaking such studies, clinicians would be able to select the proper flow rates when using NHF for children with ranging severities of OSA.

As mentioned in Chapter 3, with a single flow rate of 20 L/min, McGinley *et al* were able to improve OSA conditions in children who required an average CPAP of 9 cmH_2O (McGinley *et al*., 2009). Their findings indicate that other mechanisms of NHF may prove beneficial in treating OSA, thus reducing the needed levels of positive airway pressures to keep the airways open. One such mechanism could be the improved dead space washout of NHF therapy compared to that of CPAP therapy. Consequently, further investigations into the benefits of improved gas washout during OSA treatment using NHF should be conducted.

Lastly, since the study conducted in Chapter 3 was an *in vitro* one, the comfort of NHF was not assessed in the target age group. McGinley *et al* and Amaddeo *et al* both found improved adherence to NHF therapy for children who were intolerant of CPAP (Amaddeo *et al*., 2019; McGinley *et al*., 2009). However, these studies also used only one flow rate for NHF, 20 L/min. For this reason, a study to assess comfort involving increasing flow rates for NHF in children is required.

These future studies would help to build upon the results of the present thesis, with the ultimate goal of increasing treatment options for individuals with OSA who are having difficulties using current therapies.

Works Cited

Ahn YM. Treatment of obstructive sleep apnea in children. *Korean J Pediatr* 2010; 53: 872-879.

Alsubie HS, BaHammam AS. Obstructive Sleep Apnoea: Children are not little Adults. *Paediatric Respiratory Reviews* 2017; 21: 72-79.

Amaddeo A, Khirani S, Frapin A, Teng T, Griffon L, Fauroux B. High-flow nasal cannula for children not compliant with continuous positive airway pressure. *Sleep Medicine* 2019; 63: 24-28.

Andersen IG, Holm J-C, Homøe P. Obstructive sleep apnea in obese children and adolescents, treatment methods and outcome of treatment – A systematic review. *International Journal of Pediatric Otorhinolaryngology* 2016; 87: 190-197.

Bakker JP, Neill AM, Campbell AJ. Nasal versus oronasal continuous positive airway pressure masks for obstructive sleep apnea: a pilot investigation of pressure requirement, residual disease, and leak. *Sleep Breath* 2012; 16: 709-716.

Baumert M, Pamula Y, Martin J, Kennedy D, Ganesan A, Kabir M, Kohler M, Immanuel SA. The effect of adenotonsillectomy for childhood sleep apnoea on cardiorespiratory control. *ERJ Open Research* 2016; 2: 00003-02016.

Bhattacharjee R, Benjafield AV, Armitstead J, Cistulli PA, Nunez CM, Pepin J-LD, Woehrle H, Yan Y, Malhotra A. Adherence in children using positive airway pressure therapy: a big-data analysis. *The Lancet Digital Health* 2020; 2: e94-e101.

Bhattacharjee R, Kheirandish-Gozal L, Pillar G, Gozal D. Cardiovascular Complications of Obstructive Sleep Apnea Syndrome: Evidence from Children. *Progress in Cardiovascular Diseases* 2009; 51: 416-433.

Castro-Codesal ML, Olmstead DL, MacLean JE. Mask interfaces for home non-invasive ventilation in infants and children. *Paediatric Respiratory Reviews* 2019; 32: 66-72.

Çengel YA, Cimbala JM. Fluid mechanics: Fundamentals and applications. Boston: McGraw-HillHigher Education; 2006

Chan J, Edman JC, Koltai PJ. Obstructive sleep apnea in children. *Am Fam Physician* 2004; 69: 1147-1154.

Cheng YL, Hsu DY, Lee HC, Bien MY. Clinical verification of patients with obstructive sleep apnea provided with a customized cushion for continuous positive airway pressure. *J Prosthet Dent* 2015; 113: 29-34.e21.

Daniel J. Sampling Essentials: Practical Guidelines for Making Sampling Choices. Thousand Oaks, California: SAGE Publications, Inc.; 2012.

Donovan LM, Boeder S, Malhotra A, Patel SR. New developments in the use of positive airway pressure for obstructive sleep apnea. *J Thorac Dis* 2015; 7: 1323-1342.

Duarte RLM, Mendes BA, Oliveira-e-Sá TS, Magalhães-da-Silveira FJ, Gozal D. Nasal versus oronasal mask in patients under auto-adjusting continuous positive airway pressure titration: a real-life study. *European Archives of Oto-Rhino-Laryngology* 2020.

Duong K, Glover J, Perry AC, Olmstead D, Ungrin M, Colarusso P, MacLean JE, Martin AR. Feasibility of three-dimensional facial imaging and printing for producing customised nasal masks for continuous positive airway pressure. *ERJ Open Research* 2021; 7: 00632-02020.

Dysart K, Miller TL, Wolfson MR, Shaffer TH. Research in high flow therapy: Mechanisms of action. *Respiratory Medicine* 2009; 103: 1400-1405.

Gozal D, O'Brien LM. Snoring and obstructive sleep apnoea in children: Why should we treat? *Paediatric Respiratory Reviews* 2004; 5: S371-S376.

Guralnick AS, Pant M, Minhaj M, Sweitzer BJ, Mokhlesi B. CPAP adherence in patients with newly diagnosed obstructive sleep apnea prior to elective surgery. *J Clin Sleep Med* 2012; 8: 501-506.

Hawkins S, Huston S, Campbell K, Halbower A. High-Flow, Heated, Humidified Air Via Nasal Cannula Treats CPAP-Intolerant Children With Obstructive Sleep Apnea. *Journal of Clinical Sleep Medicine* 2017; 13: 981-989.

Hawkins SMM, Jensen EL, Simon SL, Friedman NR. Correlates of Pediatric CPAP Adherence. *Journal of Clinical Sleep Medicine* 2016; 12: 879-884.

Immanuel SA, Pamula Y, Kohler M, Martin J, Kennedy D, Kabir MM, Saint DA, Baumert M. Respiratory timing and variability during sleep in children with sleep-disordered breathing. *Journal of Applied Physiology* 2012; 113: 1635-1642.

Ingram DG, Singh AV, Ehsan Z, Birnbaum BF. Obstructive Sleep Apnea and Pulmonary Hypertension in Children. *Paediatric Respiratory Reviews* 2017; 23: 33-39.

Katz IM, Martin AR, Muller P-A, Terzibachi K, Feng C-H, Caillibotte G, Sandeau J, Texereau J. The ventilation distribution of helium–oxygen mixtures and the role of inertial losses in the presence of heterogeneous airway obstructions. *Journal of Biomechanics* 2011; 44: 1137-1143.

Kirkness JP, Verma M, McGinley BM, Erlacher M, Schwartz AR, Smith PL, Wheatley JR, Patil SP, Amis TC, Schneider H. Pitot-tube flowmeter for quantification of airflow during sleep. *Physiol Meas* 2011; 32: 223-237.

Léger D, Stepnowsky C. The economic and societal burden of excessive daytime sleepiness in patients with obstructive sleep apnea. *Sleep Medicine Reviews* 2020; 51: 101275.

Machaalani R, Evans CA, Waters KA. Objective adherence to positive airway pressure therapy in an Australian paediatric cohort. *Sleep and Breathing* 2016; 20: 1327-1336.

Marcus CL, Brooks LJ, Ward SD, Draper KA, Gozal D, Halbower AC, Jones J, Lehmann C, Schechter MS, Sheldon S, Shiffman RN, Spruyt K. Diagnosis and Management of Childhood Obstructive Sleep Apnea Syndrome. *Pediatrics* 2012; 130: e714.

Marcus CL, Rosen G, Ward SLD, Halbower AC, Sterni L, Lutz J, Stading PJ, Bolduc D, Gordon N. Adherence to and Effectiveness of Positive Airway Pressure Therapy in Children With Obstructive Sleep Apnea. *Pediatrics* 2006; 117: e442.

Marcus CL, Greene MG, Carroll JL. Blood Pressure in Children with Obstructive Sleep Apnea. *American Journal of Respiratory and Critical Care Medicine* 1998; 157: 1098-1103.

Martin AR, Jackson C, Fromont S, Pont C, Katz IM, Caillobotte G. An injection and mixing element for delivery and monitoring of inhaled nitric oxide. *BioMedical Engineering OnLine* 2016; 15: 103.

Massie CA, Hart RW. Clinical Outcomes Related to Interface Type in Patients With Obstructive Sleep Apnea/Hypopnea Syndrome Who Are Using Continuous Positive Airway Pressure. *Chest* 2003; 123: 1112-1118.

McArdle N, Devereux G, Heidarnejad H, Engleman HM, Mackay TW, Douglas NJ. Long-term use of CPAP therapy for sleep apnea/hypopnea syndrome. *Am J Respir Crit Care Med* 1999; 159: 1108-1114.

McGinley B, Halbower A, Schwartz AR, Smith PL, Patil SP, Schneider H. Effect of a High-Flow Open Nasal Cannula System on Obstructive Sleep Apnea in Children. *Pediatrics* 2009; 124: 179.

Miller TL, Saberi B, Saberi S. Computational Fluid Dynamics Modeling of Extrathoracic Airway Flush: Evaluation of High Flow Nasal Cannula Design Elements. *Journal of Pulmonary and Respiratory Medicine* 2016; 6: 1-7.

Möller W, Feng S, Domanski U, Franke K-J, Celik G, Bartenstein P, Becker S, Meyer G, Schmid O, Eickelberg O, Tatkov S, Nilius G. Nasal high flow reduces dead space. *Journal of Applied Physiology* 2017; 122: 191-197.

Moore CP, Rebstock D, Katz IM, Noga ML, Caillibotte G, Finlay WH, Martin AR. The influence of flowrate and gas density on positive airway pressure for high flow nasal cannula applied to infant airway replicas. *Journal of Biomechanics* 2020; 112: 110022.

Moore CP, Katz IM, Pichelin M, Caillibotte G, Finlay WH, Martin AR. High flow nasal cannula: Influence of gas type and flow rate on airway pressure and CO2 clearance in adult nasal airway replicas. *Clinical Biomechanics* 2019; 65: 73-80.

Morrison R, Vankoevering K, Nasser H, Kashlan K, Kline S, Jensen D, Edwards S, Hassan F, Schotland H, Chervin R, Buchman S, Hollister S, Garetz S, Green G. Personalized 3D-Printed CPAP Masks Improve CPAP Effectiveness in Children with OSA and Craniofacial Anomalies. 2015.

Mulgrew AT, Ryan CF, Fleetham JA, Cheema R, Fox N, Koehoorn M, FitzGerald JM, Marra C, Ayas NT. The impact of obstructive sleep apnea and daytime sleepiness on work limitation. *Sleep Medicine* 2007; 9: 42-53.

Nixon GM, Mihai R, Verginis N, Davey MJ. Patterns of Continuous Positive Airway Pressure Adherence during the First 3 Months of Treatment in Children. *The Journal of Pediatrics* 2011; 159: 802-807.

Parke R, McGuinness S, Eccleston M. Nasal high-flow therapy delivers low level positive airway pressure. *BJA: British Journal of Anaesthesia* 2009; 103: 886-890.

Paxman T, Noga M, Finlay WH, Martin AR. Experimental evaluation of pressure drop for flows of air and heliox through upper and central conducting airway replicas of 4- to 8-year-old children. *Journal of Biomechanics* 2019; 82: 134-141.

Peppard PE, Young T, Barnet JH, Palta M, Hagen EW, Hla KM. Increased Prevalence of Sleep-Disordered Breathing in Adults. *American Journal of Epidemiology* 2013; 177: 1006-1014.

Phillips B. Sleep-disordered breathing and cardiovascular disease. *Sleep Medicine Reviews* 2005; 9: 131-140.

Pinkham M, Tatkov S. Effect of flow and cannula size on generated pressure during nasal high flow. *Critical Care* 2020; 24: 248.

Rosen D. Management of obstructive sleep apnea associated with Down syndrome and other craniofacial dysmorphologies. *Current Opinion in Pulmonary Medicine* 2011; 17: 431-436.

Rotenberg BW, Murariu D, Pang KP. Trends in CPAP adherence over twenty years of data collection: a flattened curve. *Journal of Otolaryngology - Head & Neck Surgery* 2016; 45: 43.

Rowland S, Aiyappan V, Hennessy C, Catcheside P, Chai-Coezter CL, McEvoy RD, Antic NA. Comparing the Efficacy, Mask Leak, Patient Adherence, and Patient Preference of Three

Different CPAP Interfaces to Treat Moderate-Severe Obstructive Sleep Apnea. *J Clin Sleep Med* 2018; 14: 101-108.

Salepci B, Caglayan B, Kiral N, Parmaksiz ET, Comert SS, Sarac G, Fidan A, Gungor GA. CPAP Adherence of Patients With Obstructive Sleep Apnea. *Respiratory Care* 2013; 58: 1467.

Sawyer AM, Gooneratne NS, Marcus CL, Ofer D, Richards KC, Weaver TE. A systematic review of CPAP adherence across age groups: clinical and empiric insights for developing CPAP adherence interventions. *Sleep Med Rev* 2011; 15: 343-356.

Sela M, Toledo N, Honen Y, Kimmel R. Customized Facial Constant Positive Air Pressure (CPAP) Masks. *ArXiv* 2016; abs/1609.07049.

Shapiro GK, Shapiro CM. Factors that influence CPAP adherence: an overview. *Sleep and Breathing* 2010; 14: 323-335.

Shikama M, Nakagami G, Noguchi H, Mori T, Sanada H. Development of Personalized Fitting Device With 3-Dimensional Solution for Prevention of NIV Oronasal Mask-Related Pressure Ulcers. *Respir Care* 2018; 63: 1024-1032.

Shirlaw T, Duce B, Milosavljevic J, Hanssen K, Hukins C. A randomised crossover trial comparing nasal masks with oronasal masks: No differences in therapeutic pressures or residual apnea-hypopnea indices. *Journal of Sleep Research* 2019; 28: e12760.

Sigurdson K, Ayas NTAT. The public health and safety consequences of sleep disorders. This paper is one of a selection of papers published in this Special Issue, entitled Young Investigators' Forum. *Canadian Journal of Physiology and Pharmacology* 2007; 85: 179-183.

Sivieri EM, Foglia EE, Abbasi S. Carbon dioxide washout during high flow nasal cannula versus nasal CPAP support: An in vitro study. *Pediatric Pulmonology* 2017; 52: 792-798.

Strickland SL. The Patient Experience During Noninvasive Respiratory Support. *Respiratory Care* 2019; 64: 689-700.

Tan HL, Kheirandish-Gozal L, Abel F, Gozal D. Craniofacial syndromes and sleep-related breathing disorders. *Sleep Med Rev* 2016; 27: 74-88.

Taussig LM, Harris TR, Lebowitz MD. Lung function in infants and young children: functional residual capacity, tidal volume, and respiratory rats. *Am Rev Respir Dis* 1977; 116: 233-239.

Valentin A, Subramanian S, Quan SF, Berry RB, Parthasarathy S. Air Leak is Associated with Poor Adherence to Autopap Therapy. *Sleep* 2011; 34: 801-806.

Weaver TE, Sawyer AM. Adherence to continuous positive airway pressure treatment for obstructive sleep apnoea: implications for future interventions. *Indian J Med Res* 2010; 131: 245-258.

Appendix: Additional Figures

A.1 Mask Air Leak of Preferred Commercial CPAP Mask vs Customized CPAP Mask (Loose Fit – 100g)

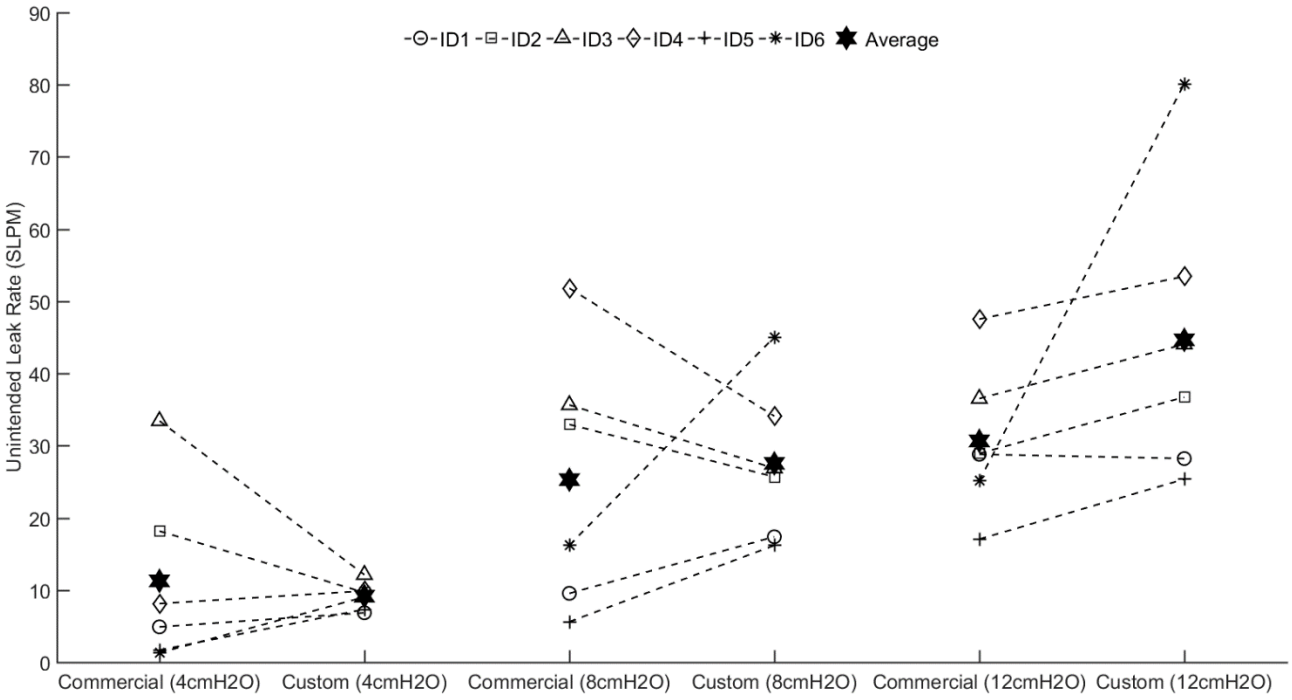

Figure A-1. Mask air leak for each subject's preferred commercial CPAP mask and their customized counterparts at a loose fit (100 g). SLPM: standard litres per minute.

A.2 Mask Air Leak of Preferred Commercial CPAP Mask vs Customized CPAP Mask (Tight Fit – 600g)

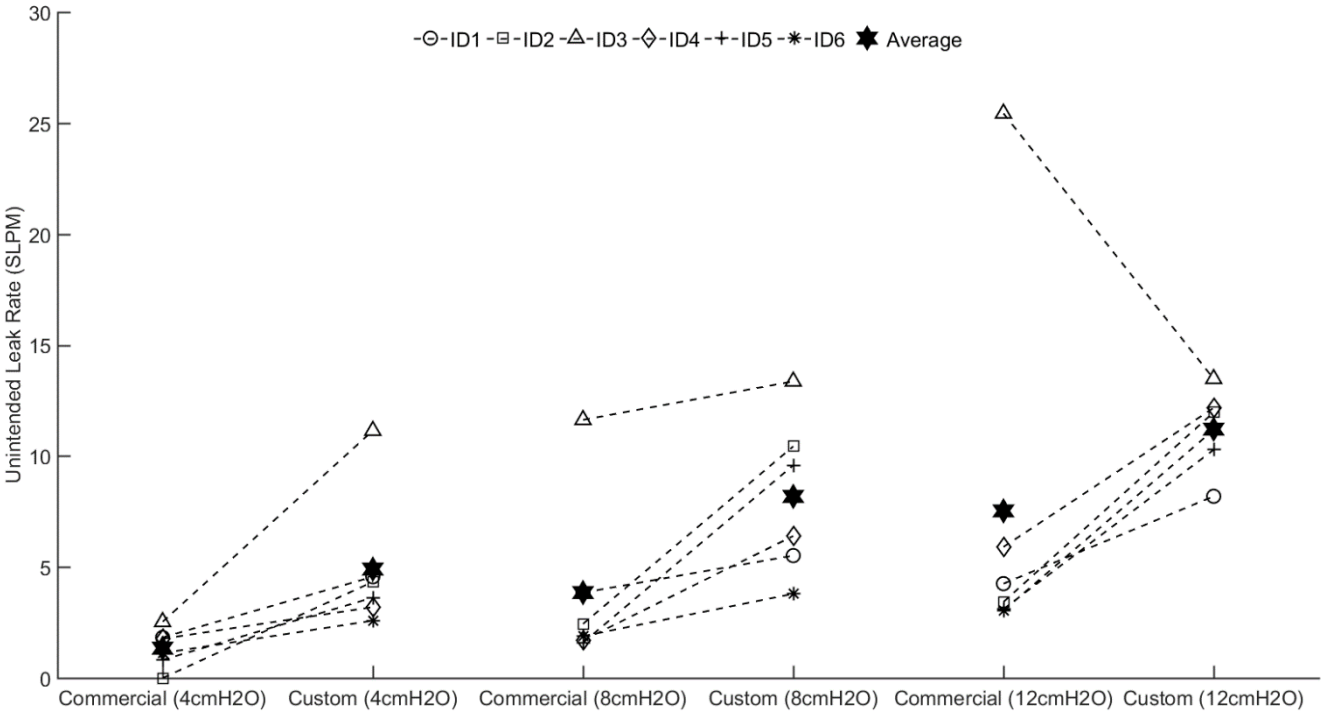

Figure A-2. Mask air leak for each subject's preferred commercial CPAP mask and their customized counterparts at a tight fit (600 g). SLPM: standard litres per minute.

A.3 Relationship between Reduction in $EtCO_2$ from Baseline and Tidal Volume/Trachea Volume

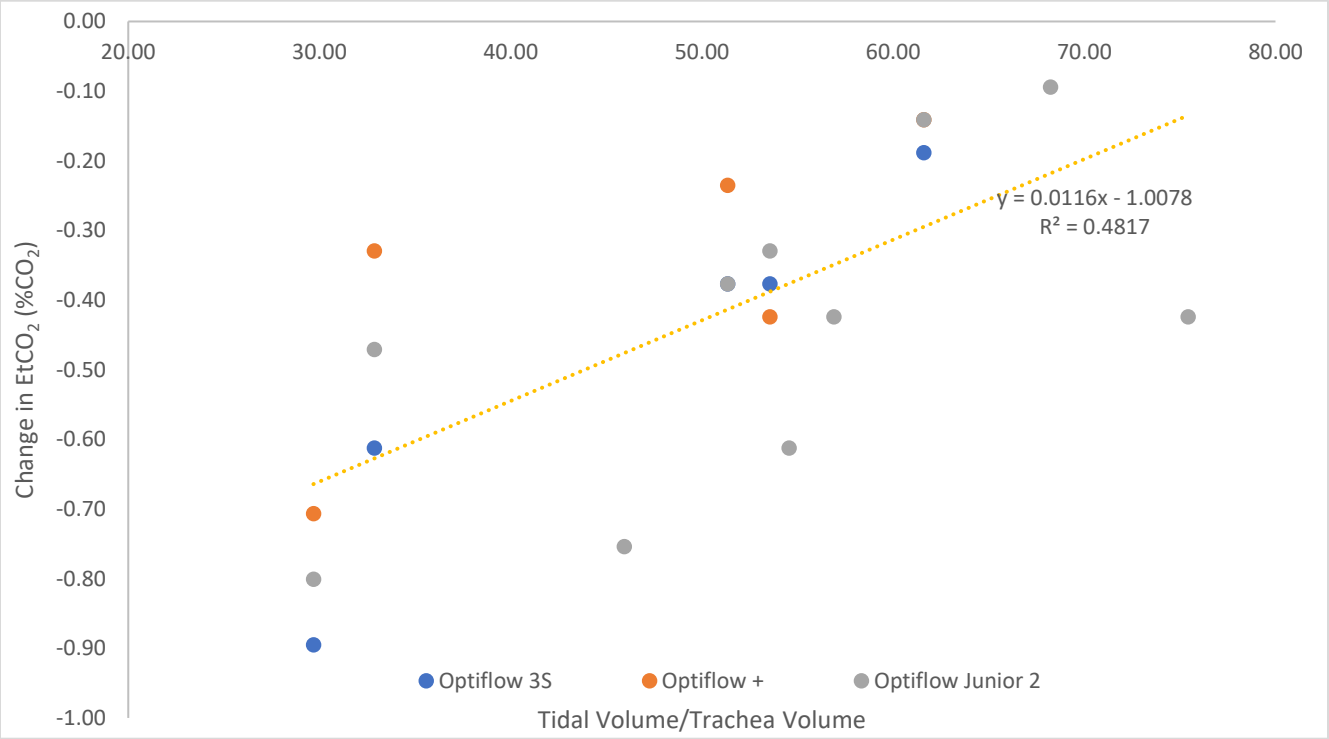

Figure A-3. Changes in $EtCO_2$ from baseline compared to the ratio of tidal volume and trachea volume for the Optiflow 3S (n = 5), Optiflow + (n = 5), and the Optiflow Junior 2 (n = 10).

A.4 Relationship between Reduction in $EtCO_2$ from Baseline and Replica Volume

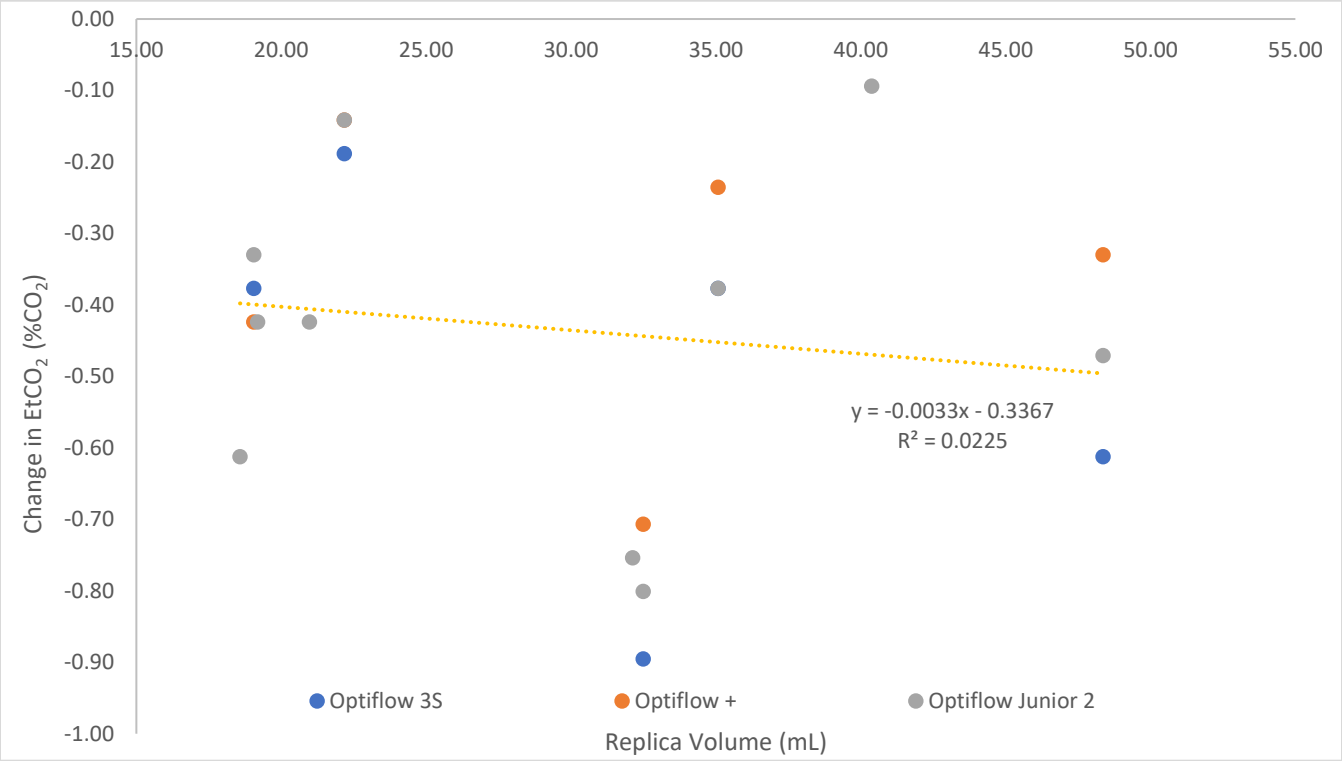

Figure A-4. Changes in $EtCO_2$ from baseline compared the replica volume for the Optiflow 3S (n = 5), Optiflow + (n = 5), and the Optiflow Junior 2 (n = 10).